uOttawa

L'Université canadienne
Canada's university

FACULTÉ DES ÉTUDES SUPÉRIEURES ET POSTDOCTORALES

uOttawa

L'Université canadienne
Canada's university

FACULTY OF GRADUATE AND POSTDOCTORAL STUDIES

Dejana Mitrovic

AUTEUR DE LA THÈSE / AUTHOR OF THESIS

M.Sc. (Biology)

GRADE / DEGREE

Department of Biology

FACULTÉ, ÉCOLE, DÉPARTEMENT / FACULTY, SCHOOL, DEPARTMENT

Physiological Consequences of Gill Remodeling in Goldfish (*Carassius auratus*) Resulting from Changes in Ambient Temperature or Oxygen Levels

TITRE DE LA THÈSE / TITLE OF THESIS

S. Perry

DIRECTEUR (DIRECTRICE) DE LA THÈSE / THESIS SUPERVISOR

CO-DIRECTEUR (CO-DIRECTRICE) DE LA THÈSE / THESIS CO-SUPERVISOR

EXAMINATEURS (EXAMINATRICES) DE LA THÈSE / THESIS EXAMINERS

C. Darveau

K. Gilmour

S. Cooke

Gary W. Slater

Le Doyen de la Faculté des études supérieures et postdoctorales / Dean of the Faculty of Graduate and Postdoctoral Studies

PHYSIOLOGICAL CONSEQUENCES OF GILL REMODELING IN GOLDFISH (*CARASSIUS AURATUS*) RESULTING FROM CHANGES IN AMBIENT TEMPERATURE OR OXYGEN LEVELS

Dejana Mitrovic

Thesis submitted to the
Faculty of Graduate and Postdoctoral Studies
University of Ottawa
in partial fulfillment of the requirements for the
M.Sc. degree in the

Ottawa-Carleton Institute of Biology

Thèse soumise à
Faculté des études supérieures et postdoctorales
Université d'Ottawa
en vue de l'obtention de la maîtrise ès sciences

L'Institut de biologie d'Ottawa-Carleton

Your file Votre référence
ISBN: 978-0-494-58227-5
Our file Notre référence
ISBN: 978-0-494-58227-5

Master of Science (2009) University of Ottawa
Biology Université d' Ottawa

Title:
Physiological consequences of gill remodeling in goldfish (*Carassius auratus*) resulting from changes in ambient temperature or oxygen levels.

Author:
Dejana Mitrovic B.Sc. (Honours) Wilfrid Laurier University

Supervisor:
Dr. Steve F. Perry – Professor, Department of Biology, University of Ottawa

Acknowledgements

First of all, I would like to thank Steve Perry, my supervisor, for having the strength and patience to take on a challenge as I am. Thank you Dr. Perry, for providing me with the opportunity to further my goals and better myself and for allowing me to grow academically. I would also like to take this opportunity to thank my committee, Dr. Katie Gilmour, Dr. Charles Darveau and Dr. Steven Cooke.

I would also like to acknowledge all my past and present lab mates from both Perry and Gilmour labs. They are all thanked for their moral support, providing pleasant working environment, social interactions and some life long friendships. Special thanks to Andrew Ochalski and Jason Popesku for technical guidance.

I would like to thank my parents for always providing encouragement and support throughout my life and studies, without them nothing would have been possible. I can not forget to thank my sister, my companion through life and my biggest fan. Finally, I would like to thank my husband, Nemanja, for supporting me, for always being understanding and patient with me and for knowing that he was much more important than any experiment even if that was not obvious.

PHYSIOLOGICAL CONSEQUENCES OF GILL REMODELING IN GOLDFISH (*CARASSIUS AURATUS*) RESULTING FROM CHANGES IN AMBIENT TEMPERATURE OR OXYGEN LEVELS

Abstract

Using two models of gill remodeling (thermally-induced and hypoxia-induced), experiments focused on the physiological consequences of changing SA (surface area) on Cl^- balance in goldfish (*Carassius auratus*). A central hypothesis was that increasing surface area (SA) associated with gill remodeling would pose a challenge to ionic regulation by promoting the obligatory trans-branchial movements of salt and water. To counter the presumed increased rates of Cl^- loss, it was reasoned that goldfish experiencing greater SA would increased the numbers or activities of the putative Cl^- transporting cells, the ionocytes.

In fish acclimated to warm water (25° C), the ionocytes were scattered along the lamellae and within the interlamellar regions of the filament. In cold water (7° C), the ionocytes were absent from the lamellae and filaments but instead restricted to the outer regions of an interlamellar cell mass (ILCM) that formed within the interlamellar channels. It was determined that in fish transferred from 25 to 7° C, the ionocytes on the outer edge of the ILCM originated predominantly from the migration of pre existing ionocytes. The greater functional lamellar surface area in the warm water acclimated fish did not result in an increase of passive branchial Cl^- efflux as was predicted on the basis of the increased paracellular movement of polyethylene glycol (PEG; 7.5 fold); these data suggest specific regulation (minimization) of Cl^- loss. Despite a reduced surface area of ionocytes in the warm acclimated fish (2103 ± 180 compared to 5219 ± 438 μm^2 mm^{-1} of filament) and higher activities of Na^+/K^+-ATPase (NKA; 1.28 ± 0.15 compared to 0.43 ± 0.06 μmol mg^{-1} protein h^{-1}), Cl^- uptake was not significantly increased to match the

elevated rate of Cl^- efflux and thus the fish at 25° C were experiencing a net loss of Cl^- across the gill which may have been countered by dietary gain of Cl^-.

Goldfish acclimated to 7° C and exposed to hypoxia (~10 mm Hg) exhibited a pronounced remodeling of the gill consisting of the retraction of the ILCM which was accompanied by a significant decrease in the surface area of ionocytes owing to a decrease in their numbers as well as size. As observed for thermally-induced remodeling, it was demonstrated that during hypoxia, pre-existing ionocytes migrated with the shrinking ILCM while a smaller proportion of newly differentiated cells appeared below the surface of the ILCM. Despite the decrease in ionocyte surface area, an elevation of Na^+/K^+-ATPase activity was suggestive of increased branchial ion transport capacity yet rates of Cl^- uptake were not any higher in the hypoxic fish. Similarly, despite an increase in functional lamellar surface area in the hypoxic fish, there was no corresponding increase in Cl^- loss or efflux of PEG. However, when hypoxic fish were returned to normoxic water for 12 h, rates of Cl^- and PEG efflux and Cl^- uptake were markedly stimulated. These data demonstrate that despite experiencing an increase in functional lamellar surface area, hypoxic goldfish limit branchial Cl^- loss likely by a hypoxia-mediated decrease in paracellular permeability that could be evident with the return of the fish to the normoxic water.

Résumé

En utilisant deux modèles de remodelage des branchies (induit thermiquement ou par hypoxie), ces expériences ont visé à examiner les conséquences physiologiques du changement de la surface branchiale sur l'équilibre du Cl^- chez le cyprin doré (*Carassius auratus*). Notre hypothèse dominante postulait qu'en augmentant la superficie de la branchie par son remodelage, l'échange ionique serait altéré dû aux mouvements obligatoires trans-branchial de l'eau et du sel. Pour contrer les augmentations de pertes de Cl^-, nous avons supposé que le cyprin doré ayant une superficie branchiale plus grande augmenterait le nombre ou l'activité des cellules transporteuses de Cl^-, les ionocyte.

Chez les poissons acclimatés à l'eau chaude (25° C), les ionocyte étaient dispersées le long des lamelles et dans les régions inter-lamellaires du filament. Dans l'eau froide (7° C), les ionocyte étaient absentes des lamelles et des filaments, mais elles étaient limitées à la périphérie de la masse de cellules inter-lamellaire (MCIL) qui se sont formés dans les canaux inter-lamellaires. Chez les poissons transférés de 25 à 7° C, les ionocyte situés à la périphérie de la MCIL provenaient principalement de la migration de CRM préexistantes. La superficie lamellaire fonctionnelle plus grande dans les poissons acclimatés pareau chaude n'a pas eu comme conséquence une augmentation de flux branchial passif de Cl comme a été prévu sur la base du plus grand mouvement paracellulaire du polyéthylène glycol(PEG; 7.5 fold); ces données suggèrent qu'il existe une régulation (minimisation) spécifique de la perte en Cl^-. Malgré une plus grande surface des ionocyte chez les poissons acclimatés à l'eau chaude (2103 ± 180comparé à 5219 ± 438 $\mu m^2\ \mu m^{-1}$) et une plus grande activité des ATPase-Na^+/K^+ (NKA; 1.28 ± 0.15 comparé à 0.43 ± 0.06 $\mu mol\ mg^{-1}$ protéine h^{-1}), l'absorption du Cl^- n'était pas augmenté

de façon significative pour équilibrer l'écoulements de Cl^- provenant des branchies. Ainsi, les poissons exposés à une eau à 25° C ont subit une perte nette de Cl^- à travers la branchie qui a pu être contrebalancé par une ingestion de Cl^- lors de la prise alimentaire.

Les cyprins dorés acclimatés à 7° C et exposés à l'hypoxie (~10 mm Hg) manifestaient un remodelage des branchies avancé qui consistait en une rétraction de la MCIL accompagné d'une augmentation significative de la surface des ionocyte due à leur prolifération. Comme observé lors du remodelage induit thermiquement, en hypoxie les ionocyte préexistantes ont migré avec la diminution de la MCIL, tandis qu'une proportion réduite des cellules nouvellement différenciées est apparu sous la surface de la CMI. En dépit de la diminution de la superficie d'ionocyte, une altitude d'activité de Na+/K+-ATPase était suggestive de la capacité branchial accrue de transport d'ionsuggérant une augmentation des capacités de transport ionique des branchies, mais les taux d'absorption de Cl^- n'était pas plus élevé chez les poissons exposé à l'hypoxie. De façon similaire, malgré une augmentation de la surface fonctionnelle des lamelles chez les poissons hypoxiques, il n'y a pas eu d'augmentation équivalente de la perte en Cl^- ou de l'absorption de PEG. Cependant, quand les poissons hypoxiques ont été replacés en eau oxygénée pour 12 heures, les taux de perte en Cl^- et PEG, ainsi que les taux d'absorption du Cl^-, étaient nettement augmentés. Ces données démontrent que malgré une augmentation de la surface fonctionnelle des lamelles, perte branchial de Cl de limite hypoxique de goldfish probablement par une diminution hypoxie-négociée de la perméabilité paracellulaire qui pourrait être évidente avec le retour des poissons à l'eau normoxique.

Table of Contents

List of Figures

List of Tables

Abbreviations

° C, degrees Celsius
BP, base pairs
DNA, deoxyribobucleic acid
FW, fresh water
ILCM, interlamellar cell mass
$J_{IN}Cl^-$, Cl^- influx
$J_{OUT}Cl^-$, Cl^- efflux
MRCs, mitochondrion rich cells
mRNA, messenger ribonucleic acid
N, number of samples or individuals
NKA, Na^+/K^+-ATPase
NKA^+, Na^+/K^+-ATPase positive cells
PO_2, partial pressure of oxygen
REAL TIME RT-PCR, real time reverse transcription PCR
SA, surface area
SEM, standard error of mean

CHAPTER 1

GENERAL INTRODUCTION

There are a number of important physiological processes whose main functional site is at the gills (Evens et al., 2005). The fish gill involvement is included in everything from environmental sensing, hormone production, acid-base balance, ion regulation, excretion of nitrogenous waste to exchange of oxygen and carbon dioxide (Evans et al., 2005). The gill is a dynamic organ that can undergo drastic and often reversible morphological changes so as to achieve optimal rates of these various functional systems. These morphological changes can be incorporated with behavioural, cardiovascular or a biochemical adjustment, in order to provide optimal conditions for varies metabolic needs (Sollid et al., 2005). The anatomy of the gill is characterized by elaborate vascular and structural systems (Nilsson, 1998) which reflect the diverse functions of this organ.

In teleosts, the gills are located on either side of the pharynx and are made up of four sets of arches that offer structural support and provide space for the blood vessels (Evans et al., 2005; Wilson & Laurent, 2002). The arches are evenly spaced and each arch extends into 2 rows of numerous filaments. These filaments are further divided into lamellae thus providing the large functional surface area (SA) that is required for gas transfer (Wilson & Laurent, 2002). The lamellae are separated by an interlamellar space Wilson & Laurent, 2002), also known as channels. It is through the interlamellar channels that water passes and where the exchange of gases and ions between the water and blood occurs. The interlamellar channels are present in most fish, but depending on environmental conditions or developmental age, these channels can be filled with an interlamellar cell mass (ILCM; Sollid et al., 2003) resulting in a loss of lamellar functional SA (see below). While not always visible, lamellae are there regardless of the amount of the ILCM present (Sollid et al., 2003).

Fish gill cell types

There are a variety of cell types within the gill epithilium including pavement cells, mucous cells, neuroepithelial cells and mitochondrion rich cells (MRCs; Evans et al., 2005; Wilson & Laurent, 2002; Perry, 1997). The MRCs are thought to be the cell types specifically involved in ionic as well as acid-base regulation. Because there are various subtypes of MRCs in fish that may transport different ions, use of the term "ionocyte" is sometimes used to denote generically all members of the MRC family (Hwang and Lee, 2007). The different ionocyte types can be distinguished on the basis of a number of factors such as location, function, blood supply as well as physical characteristics including cell thickness or cell shape (Evans et al., 2005). Distinguishing features of ionocytes are the presence of numerous mitochondria and an abundance of Na^+/K^+ ATPase enzyme, they also have extensive tubular network, they are usually found at the basal regions of the lamellae channel and more often then not they are exposed to the flow of water (Evans et al., 2005; Wilson & Laurent, 2002; Perry, 1997). Depending on the environment that a fish inhabits, these cells may change shape to reflect their changing function (Perry, 1997). In seawater the ionocytes are mostly responsible for ion excretion and posses a variety of surface topologies (Perry, 1997). While the function of the MRCs is defined in seawater, in fresh water (FW) their functions is not completely resolved, but most likely they are involved in ion uptake (Perry, 1997).

In rainbow trout (*Oncorhynchus mykiss*), the ionocytes form two subtypes (Goss et al., 2001); acid-secreting cells are thought to be involved in absorption of Na^+ while base-secreting cells are linked to Cl^- uptake (Perry, 1997; Perry et al., 2003). These subtypes of ionocytes are also distinguished based on their location and membrane

proterties (Perry, 1997). The relative proportions of these ionocyte subtypes may depend on the environment in which the fish is found (Perry, 1997). In addition to trout, phenotypically different populations of ionocytes have been identified in only a few teleost fish species including ; killifish (*Fundulus heteroclitus*; Laurent et al., 2006), zebrafish (*Danio rerio*; Hwang and Lee, 2007) and tilapia (*Oreochromis mossambicus*; Hiroi et al., 2008). The portion of the exposed surface of the ionocyte to the water seems to depend on the activity of these cells given the fixed environmental conditions as well as on the intrinsic leakiness of the gill to the ions in question (Perry, 1997).

Gas transfer

Gas transfer occurs by diffusion at the level of lamellae and is driven by the partial gradients of the gases between the blood and the water (Perry et al., 2003). The rate of exchange is also dependent on the specific properties of gases including their diffusivity and capacitance. Due to its high capacitance, CO_2 diffuses across the respiratory barrier more rapidly than O_2. Also, gas exchange is related to the SA of the exchange surface and the thickness of the diffusion barrier found between the water and blood. It is these two physical characteristics of the gill together with changing the ventilation and perfusion rates that can be altered in order to match gas transfer requirements with the metabolic demands (Evans et al., 2005). Both the functional SA of the gill and the thickness of the diffusion barrier are positively impacted by the reduction of the ILCM elicited by an increase in temperature (Sollid et al., 2003, 2005). Conversely, the proliferation of lamellar ionocytes may result in a thickening of the lamellar diffusion barrier negatively influencing respiratory gas transfer. The balance

between all these characteristics is achieved in order for the gill to perform at its optimal level.

Ionic regulation

In FW, fish must cope with continual passive ion loss due to the negative gradient of ions in the water compared to the fish blood, thus electrolyte homeostasis is achieved by actively pumping ions across the gill epithelium into the blood stream (Marshall and Grosell, 2006). Ongoing research is focusing on the specific cell types involved in uptake of the various ions through the gill epithelium. Cl^- uptake is believed to occur across an unidentified apical membrane Cl^-/HCO_3^- exchanger followed by transfer out of the cell through a basolateral anion channel (Perry et al., 2003a; Perry et al., 2003b; Evans et al., 2005; Perry and Gilmour, 2006; Marshall and Grosell, 2006; Tresguerres et al., 2006; Claiborne et al., 2008). Cl^- uptake is thought to be localized to a subset of ionocytes that are believed to be functionally analogous to the base secreting (B-type) intercalated cells of the mammalian collecting duct (Perry et al., 2003a; Perry et al., 2003b; Evans et al., 2005; Perry and Gilmour, 2006; Marshall and Grosell, 2006; Tresguerres et al., 2006; Claiborne et al., 2008). This is supported by the evidence that in ion poor water, there is a proliferation of the branchial chloride cell, ionocyte, which would indicate an increased transporting capacity for Cl^- ions (Perry, 1997). Another subset of ionocytes is believed to be analogous to the acid secreting (A-type) intercalated cells of the collecting duct in which an apical membrane Na^+/H^+ exchanger and/or Na^+ channel/V-ATPase linked process act to absorb Na^+ (Reid et al., 2003; Lin et al., 2006;

Horng et al., 2007; Parks et al., 2007; Yan et al., 2007; Hwang and Lee, 2007). Different sub-populations of ionocytes have not yet been identified in goldfish gill.

Functional SA and the osmoregulatory compromise

A large functional SA is necessary to sustain adequate rates of gas transfer across the gills. Gas transfer rates across the gills can vary due to a number of factors, like temperature, hypoxia, fish metabolism, developmental stages and exercise levels (Nilsson, 2007). However, factors that result in high rates of branchial gas transfer (e.g. high surface area) also result in high rates of passive loss of salts and entry of water across the gill in fresh water fish due to the water chemistry. In order the re-establish the necessary equilibrium all the salts that have been lost need to be actively reabsorbed. Because the cost of actively absorbing salts in FW is high (Perry, 1997), gill SA typically is kept as low as possible but still sufficient to meet gas transfer requirements. The need to enlarge SA for gas transfer conflicts with a need to reduce SA to minimize obligatory movements of salt and water. The osmorespiratory compromise is a term used to emphasise the matchup between the need for large SA and high costs for active absorption of ions. Thus, by maintaining surface area as low as is possible, while still being able to accomplish necessary gas transfer, the obligatory movements of salt and water across the gill are reduced thereby lowering the energetic costs of ion regulation.

Effects of temperature on the fish gill

Previous research performed on crucian carp and goldfish indicated that gill SA varies according to environmental conditions, resulting in possible alterations of gas

transfer. Sollid et al., (2003; 2005) demonstrated that in crucian carp exposed to cold water, SA of the gills was much lower when it was compared to the fish gill exposed to warm water. Specifically, it was demonstrated that at low temperatures, the gill lamellae are largely covered by an interlamellar cell mass (ILCM) that limits their exposure to water (Sollid et al., 2003; 2005). The exposure to different temperatures can occur with changing of the seasons, sudden ice melts or after profound rain pour. Sudden change in temperature of the water can also be linked to the size of the pond that the fish might be found in as shallow water can be more affected by sun and wind. Though the exact signaling mechanisms are unknown, gill remodeling (at least in crucian carp) via the invasion or retraction of an ILCM occurs by cell proliferation and apoptosis, respectively (Sollid et al., 2003).

With reduced SA, the energy expended on osmoregulation presumably will be decreased. Low ambient temperature will also depress metabolism and fish movements and excercise thus allowing lower rates of O_2 uptake to sustain activity (Sollid and Nilsson, 2006). With the demand for oxygen reduced and an increased solubility of O_2 in the cold water, the fish can cover its gills without jeopardizing its survival chances. With the lamellae covered, the functional SA will be low, so to minimize the cost of ionic regulation. Covering of the lamellae has another advantage as smaller SA reduces the accessibility of the fish to pathogens and toxins present in the environment (Sollid and Nilsson, 2006).

In crucian carp and goldfish acclimated to higher temperatures, the ILCM is retracted thereby exposing the lamellae and increasing the SA (Sollid et al., 2003; 2005). With the lamellae exposed, more epithelial cells will be in contact with water and more

O_2 can be obtained. While the increases in functional SA should be able to provide the higher levels of O_2, these changes will also affect the cost of osmoregulation because water gain and ion loss will increase owing to increasing SA. Thus with the increase of the functional SA there will be an increase in the actively pumping of the ions across the gill epithelium and this should be evident in the upregulation of the ionocytes thought to be responsible for ion absorption. The removal of the ILCM should also have an effect on the size and number of the ionocytes, assuming that they become exposed to the water flow with the removal of the ILCM. Regardless of the mechanisms behind the changes of the ILCM, this phenomenon is reversible; the lamellae are covered once again as the fish is exposed to cold water (Sollid and Nilsson, 2006).

Effects of hypoxia on the fish gill

Several animals can survive in environments with minimal or no O_2 for prolonged periods of time (Stensløkken et al., 2008; Scott et al., 2008; Brauner et al., 2004; De Fraga et al., 2004; Nilsson, 2001). Fish can face hypoxia in snow cover lakes where oxygen can be depleted over time or algal booms may result in lower oxygen concentration within a pond. Just as animals are different so are their tactics for hypoxia adaptations, and the ways that an animal might adapt to hypoxia can have a profound effect on its development and functioning. In the case of gill remodeling, the morphological changes may be permanent as in the developmental maturation of *Arapaima gigas* (Brauner et al., 2004), or reversible as in crucian carp (Sollid et al., 2005; 2003), goldfish (Sollid et al., 2005) and mangrove killifish (*Kryptolebias marmoratus;* Ong et al., 2007). Goldfish and crucian carp are particularly interesting because of their

large hepatic glycogen reserves and their production of ethanol (instead of lactic acid) as the end product of anaerobic metabolism thus they do not experience toxic sideeffects of lactic acid (Shoubridge and Hochachka, 1980). Both species drastically reduce their metabolic rates in hypoxic situations but do not enter a comatose state that is observed in the western painted turtle (Nilsson, 2001). Eventually their survival depends on the amount of glycogen they posses and thus it is advantageous to postpone the utilization of these stores and reliance on the anaerobic metabolism. In crucian carp, prolonging aerobic metabolism is accomplished by changing the morphology of the fish gills during hypoxia to allow greater SA for O_2 uptake (Sollid et al., 2003, 2005). However, by increasing surface area for O_2 uptake the cost of osmoregulation is likely to increase (see above).

Previous studies performed on crucian carp indicate that in normoxic conditions this species is able to maintain a low functional SA by having an extensive ILCM covering its gills, thus when faces with a hypoxic situation it has an ability to alter its gills and profoundly increase the functional SA in order to benefit O_2 uptake (Nilsson, 2007; Sollid and Nilsson, 2006; Sollid et al., 2003; Sollid et al., 2005). The increase in the functional SA is achieved by retraction of the ILCM thus exposing previously covered regions of the lamellae (Sollid et al., 2003). While the increase in SA is beneficial for O_2 uptake, it is likely that it will also increase the cost of osmotic and ion regulation, thus might seem counterproductive (Gonzales and McDonald, 1992; Randall et al., 1972). There will need to be increase efforts of active pumping of ions across the gill epithelium in order to offset the ion loss that will occur due to the increasing SA. The balance that exists between the need to minimize functional SA for prevention of

high cost ionic regulation and the ability to maximize functional surface area for gas transfer is termed osmorespiratory compromise (Randall et al., 1972). Just like in temperature situation, here too needs to exist an trade off to optimally serve both needs of the fish.

Aim of the thesis

This thesis focuses on the consequences of gill remodeling in goldfish on Cl^- balance. Chapter 2 addresses the effects of thermally induced gill remodeling while Chapter 3 examines hypoxia-induced gill remodeling; two hypotheses are investigated:

1. An increase in lamellar functional SA in fish acclimated to warmer water or hypoxia (while presumably beneficial to O_2 uptake) will promote Cl^- loss that will be matched by equivalent increases in Cl^- uptake owing to an augmentation of branchial ion transport capacity.
2. The ionocytes migrate with the ILCM to remain perpetually exposed to the water so as to maintain the potential for Cl^- uptake.

CHAPTER 2

THE EFFECTS OF THERMALLY INDUCED GILL REMODELING ON CHLORIDE BALANCE IN GOLDFISH (*CARASSIUS AURATUS*)

Chapter 2 is based on a manuscript that is in press in Journal of Experimental Biology

D. Mitrovic and S. F. Perry (2009). The effects of thermally induced gill remodeling on ionocyte distribution and branchial chloride fluxes in goldfish (*Carassius auratus*). *J.Exp.Biol.* In Press.

Abstract

Experiments were performed to evaluate the effects of temperature induced changes in functional lamellar surface area on the distribution of ionocytes and chloride balance in goldfish (*Carassius auratus*). In fish acclimated to warm water (25° C), the ionocytes were scattered along the lamellae and within the interlamellar regions of the filament. In cold water (7° C), the ionocytes were largely absent from the lamellae and filaments but instead were mostly confined to the outer regions of an interlamellar cell mass (ILCM) that formed within the interlamellar channels. Using a "time-differential double fluorescent staining technique" (Katoh and Kaneko, 2003), it was determined that in fish transferred from 25° to 7° C, the ionocytes on the outer edge of (and within) the ILCM originated predominantly from the migration of pre existing ionocytes and to a lesser extent from the differentiation of progenitor cells. Despite the greater functional lamellar surface area in the warm water acclimated fish, there was no associated significant increase in passive branchial Cl^- efflux. Because the paracellular efflux of polyethylene glycol was increased 7.5-fold at warmer temperature, it would suggest that goldfish specifically regulate (minimize) Cl^- loss that otherwise would accompany the increasing functional lamellar surface area.

In contrast to predictions, the numbers and sizes of individual ionocytes were inversely related to functional lamellar surface area resulting in a markedly greater ionocyte surface area in fish acclimated to cold water (5219 ± 438 compared to 2103 ± 180 $\mu m^2\ mm^{-1}$ of filament). Paradoxically, the activity of Na^+/K^+-ATPase was also lower in the cold water fish (0.43 ± 0.06 compared to 1.28 ± 0.15 $\mu mol\ mg^{-1}$ protein h^{-1}) despite

the greater ionocyte surface area. There were no statistically significant differences in the rates of Cl^- uptake in the two groups of fish despite the differences in ionocyte abundance. It is possible that to maintain normal rates of Cl^- uptake, a greater ionocyte surface area is required in the cold water fish that possess an ILCM because of the unfavourable positioning of the ionocyte on and within the ILCM, a structure lacking any obvious blood supply.

Introduction

The fish gill is the site of numerous physiological processes including chemoreception (Burleson et al., 1992; Burleson, 1995; Jonz et al., 2004; Burleson et al., 2006; Gilmour and Perry, 2007), hormone metabolism (Olson, 1998; Olson, 2002), acid-base regulation (Claiborne, 1998; Perry and Gilmour, 2006), excretion of nitrogenous wastes (Wood, 1993; Wright, 1995) gas exchange (Randall and Daxboeck, 1984; Perry and McDonald, 1993; Gilmour, 1997; Perry and Gilmour, 2002; Nikinmaa, 2006) and ionic regulation (Goss et al., 1992; Evans et al., 1999; Marshall and Grosell, 2006; Hwang and Lee, 2007). Elements of these physiological functions, in particular the diffusive component of gas transfer, require a large functional surface area. In the fish gill, surface area is markedly increased by the presence of thousands of highly vascularized lamellae that project from gill filaments (Laurent and Dunel, 1980; Laurent, 1984; Wilson and Laurent, 2002). The spaces between adjacent lamellae through which ventilatory water flows are termed the interlamellar channels. Functional surface area is labile and typically is adjusted in a regulated fashion according to metabolic requirements or environmental conditions. There are distinct advantages associated with such dynamic adjustments of surface area. Essentially, factors favouring high rates of branchial gas transfer (e.g. high surface area) will also result in higher rates of obligatory salt and water movements across the gill (Randall et al., 1972; Gonzales and McDonald, 1992). Because of the relatively high costs of actively absorbing salts in freshwater (FW) and actively excreting salts in seawater, functional surface area is matched to gas transfer requirements; a phenomenon termed the osmorespiratory compromise. Thus, by

maintaining surface area as low as is possible, the obligatory movements of salt and water across the gill are reduced and hence the energetic costs of ion pumping are minimized. Acute changes in functional surface area can be achieved by recruiting previously unperfused lamellae (lamellar recruitment) or by more uniformly perfusing individual lamellae (Booth, 1979; Farrell et al., 1980). Chronic (hours to days) and occasionally extreme changes in functional surface area are accomplished in some species by physical covering/uncovering of lamellae (Sollid et al., 2003; Metz et al.,2003; Brauner et al., 2004; Sollid et al., 2005; Ong et al., 2007) (see reviews by Sollid and Nilsson, 2006; Nilsson, 2007). Crucian carp (*Carassius carassius*), goldfish (*Carassius auratus*) and mangrove killifish (*Kryptolebias marmoratus*) exhibit reversible gill remodeling in accordance with changes in O_2 demand or availability, while *Arapaima gigas* exhibits a permanent remodeling of lamellar structure in association with a developmental transition from water- to air-breathing (Brauner et al., 2004). Though the signalling mechanisms are unknown, gill remodeling is accomplished by the invasion or retraction of an interlamellar cell mass (ILCM) by cell proliferation and apoptosis, respectively (Sollid et al., 2003).

In the present study we have focused on the consequences of gill remodeling on Cl^- balance. In goldfish, the ILCM is present in fish acclimated to cold normoxic water, but is retracted in fish exposed to waters of increasing temperature (Sollid et al., 2005). Thus, an increased surface area at higher temperature would be expected to increase passive Cl^- loss and therefore would need to be matched by equivalent increases in Cl^- uptake, necessitating an increase in the ion transporting capacity of the gill. In FW fish, the mitochondrion rich cell (MRC) or FW chloride cell (Perry, 1997) is believed to be the

cell type responsible for Cl^- uptake (Perry, 1997; Perry et al., 2003b; Tresguerres et al., 2006). Because there are numerous subtypes of MRC in fish that may transport different ions, use of the term "ionocyte" is gaining favour to denote generically all members of the MRC family (Hwang and Lee, 2007). With this background, we hypothesize in the present study that increased functional lamellar surface area in goldfish acclimated to warm water will increase Cl^- efflux that will be matched by increased Cl^- uptake owing to an increase in the numbers of ionocytes. Conversely, a loss of Cl^- uptake capacity in goldfish exhibiting an ILCM is expected not only to match the predicted reduction in Cl^- efflux, but also because the ionocytes typically located at the base of filaments within the interlamellar regions might become inoperable owing to their covering by the ILCM. Under such conditions, a substantial loss of Cl^- uptake capacity might be expected. Thus, our second hypothesis is that ionocytes migrate with the ILCM to remain perpetually exposed to the water so as to maintain the potential for Cl^- uptake.

Materials and Methods

Experimental animals

All experiments were performed according to the University of Ottawa institutional guidelines which comply with those of the Canadian Council on Animal Care (CCAC). Goldfish, *Carassius auratus* weighing on average 23.9 ± 0.4 g, N = 207) were obtained from Along's International (Mississauga, Canada). They were first acclimated to 18° C in large fibreglass tanks filled with dechlorinated tap water. After at least one week, temperatures were either increased or decreased 2° C per day to achieve final acclimation temperatures of 7° or 25° C. Animals were kept in the facility under a 12h: 12h light: dark photoperiod and were fed once a day with commercial food pellets. Fish were kept under such conditions for at least two weeks prior to their use in experiments. Twenty four hours prior to any experiment, fish (including controls) were moved from their holding tanks to individual boxes (approximately 600 ml water volume) provided with flowing aerated water at the appropriate acclimation temperature; fish were not fed.

At the end of each experiment, fish were killed by anaesthetic overdose using a solution of benzocaine (ethyl-*P*-amino-benzoate, 2.4 X 10^{-4} mol l^{-1}, Sigma, St Louis, MO, USA) and gill tissue was removed and processed for light microscopy, immunocytochemistry, Na^+/K^+-ATPase (NKA) activity and real-time reverse transcription PCR (real time RT-PCR). For some experiments, blood and water samples were also collected.

Light microscopy and immunocytochemistry

Upon removal of the gill arches, filaments from arches 1 and 2 (left side) were placed into a solution of zinc iodide-2% osmium tetroxide (3:1 ratio) for at least 24 h at room temperature (Garcia-Romeu and Masoni, 1970). The samples were then cryo-protected using 15% sucrose (12 h) followed by 30% sucrose. All samples were stored in 30% sucrose at 4° C prior to use. The gills were embedded in OCT cryosectioning medium (VWR), incubated for 20 min and sectioned horizontally (10 μm section) using a cryostat (Leica CM 1850 Laboratories Eq., Germany). Sections were placed on microscopy slides (Superfrost Plus; Fisher) and mounted with 60% glycerol under a cover slip.

For immunocytochemistry, gill filaments from arches 1 and 2 (right side) were placed directly into 4% paraformaldehyde and left overnight at 4° C. Tissues were cryo-protected in sucrose and sectioned (10 μm thick sections) using a cryostat (see above). Sections were placed on microscopy slides (Superfrost Plus; Fisher) and allowed to incubate for 1 h at room temperature prior to being stored at 4°C until required. Following 3 X 5 min washes with PBST (0.1M phosphate buffered saline, 0.3% Triton-X 100) and blocking with sheep serum (1:10 dilution, Sigma) for 1 h, sections were incubated for 2 h at room temperature with primary antibody: α5 (1:100), a mouse monoclonal antibody against the α1 sub-unit of chicken Na^+/K^+-ATPase (University of Iowa Hybridoma Bank). The α5 antibody has been used successfully for immunocytochemistry in numerous vertebrate species including fish (e.g. Wilson et al., 2000). For negative controls, sections were incubated with 1X PBST buffer lacking primary antibody. Immunofluorescence was detected after incubating the sections with a

1:400 dilution of Alexa Fluor-546 coupled to goat anti-mouse IgG (Fisher, Ottawa, ON, Canada) for 1 h. After washing (3 x 10 min in 0.1X PBS), sections were mounted in Vectashield mounting medium (Vector Labs, Canada) and cover slipped.

For each fish, 2 gill sections were examined using light or epifluorescence microscopy. Photos (4 per fish) from randomly selected areas of the mid regions of the gill filament were taken at 40X magnification. Photos were taken using an Axiophot (Zeiss, Germany) microscope, Olympus DP70 digital microscope camera and Image Pro Plus software Version 6.0 (Media Cybernetics Inc., Bethesda, USA). Digital images were analyzed using web-based imaging software (Image J, Waine Rasband, Maryland, USA) to determine morphological variables including numbers and two-dimensional surface areas of ionocyes (as identified using zinc$$ iodide-osmium tetroxide staining or NKA immunofluorescence) and the relative surface area of the ILCM.

Na^+/K^+ ATPase activity

The third gill arch from each fish was added to SEI buffer (150 mmol l^{-1} sucrose, 10 mmol l^{-1} EDTA, 50 mmol l^{-1}imidazole), frozen in liquid N_2 and stored at -80° C. Na^+/K^+ ATPase activity was determined (in triplicate) in the supernatant of homogenized samples using a spectrophotometric microplate assay according to McCormick (1993). Ouabain-sensitive ATPase activity was measured and expressed in units of μmoles ADP mg^{-1} protein h^{-1} and compared to ATPase activity in the absence of ouabain. Protein was determined using the bichinchonic acid method (BIORAD) according to the instructions of the manufacturer.

Real-time RT-PCR

Total RNA was extracted from 100 mg of gill tissue using TRIzol Reagent (Invitrogen) and re-suspended in 40 µl of nuclease-free water. Reverse transcription was performed using the Revertaid H Minus M-MuLV reverse transcriptase enzyme according to the protocol for cDNA synthesis provided by the manufacturer (Fermentas, Life Sciences). The following modifications were made: the final reaction volume was 20 µl and 2 µl of RNA was used with 0.2 µg or random hexamer primers. An MX 3000 Multiplex Quantitative PCR System (Stratagene) and Brilliant SYBR Green QPCR Master Mix (Stratagene) were used for the real-time RT-PCR as per the instructions of the manufacturer with slight modifications: the total reaction volume was adjusted to 12.5 µl, 1 µl of cDNA template was used and final primer concentrations were 100 nmol l^{-1}. Annealing and extension temperatures were 55° C (1 min) and 72° C (1min) for 40 cycles. All the primers used for real time PCR (including the reference gene 18S ribosomal RNA) were designed using web-based software (primer3; http://frodo.wi.mit.edu/cgi-bin/primer3/primer3_www.cgi). To obtain homologous primers to amplify goldfish NKA, a 485 bp nucleotide sequence obtained from a BLAST search of GenBank (Accession FG392680) was used to provide a product size of 123 bp.

NKA 1α (09a01);

Forward primer 5'-CGAGGTACCGTCACCATTCT-3',

Reverse primer 5'-GTCTGTTTTGGGGTTTCTGG-3'

Primers for 18S ribosomal RNA were designed from a 551 bp nucleotide sequence obtained from a BLAST search of GenBank (Accession AF047349);

Forward primer 5′-GAGCCTGAGAAACGGCTACC-3′,

Reverse primer 5′-CCATGGGTTTAGATATGCTC-3′

The specificity of the primers was verified by cloning and sequencing of the amplified products. To ensure that residual genomic DNA was not being amplified, control experiments were performed in which reverse transcriptase was omitted during cDNA synthesis. Relative expression of mRNA levels was determined (using 18S RNA as an endogenous standard) by a modification of the Δ-Δ Ct method (Pfaffl, 2001). Amplification efficiencies were determined from standard curves generated by serial dilution of plasmid DNA.

"Time-differential double fluorescent staining" of ionocytes

To determine whether ionocytes were migrating with the ILCM during temperature change or alternatively appearing as newly differentiated ionocytes, the "time-differential double fluorescent staining" technique of Katoh and Kaneko (2003) was adopted with the following modifications. Only one ^{TM}MitoTracker (MitoTracker Red CMXRos, Molecular Probes) was used; fish were exposed to this fluorescent mitochondria-specific dye for 4 h (1 μmol l^{-1}) at a water temperature of 25° C. Fish were then exposed to running water and the temperature of the water was gradually reduced to 7° C over the next two weeks; control fish were maintained at 7° C for two weeks. After 2 weeks, fish were euthanized (see above) and gill tissue was removed, fixed and sectioned for immunocytochemistry as described previously while allowing as little exposure to light as possible. To detect NKA-enriched cells, the α5 monoclonal antibody was used in conjunction with the secondary antibody Alexa Fluor-488 (green) coupled to

goat anti-mouse IgG (Fisher, Ottawa, ON, Canada). Because we previously demonstrated that all NKA-enriched cells in goldfish will stain positively with ^{TM}MitoTracker (unpublished observations), this protocol allows time-dependent differential labelling of the ionocytes. Thus, if a cell is stained both red and green, it existed prior to the onset of temperature change whereas if a cell is stained only green (^{TM}MitoTracker negative, NKA positive), it is assumed that it is a new ionocyte that did not exist at the beginning of the experiment.

Chloride fluxes and plasma analysis

To assess the effects of temperature change and gill remodeling on Cl^- efflux ($J_{OUT}Cl^-$), fish were lightly anesthetised and injected intraperitoneally with 40 μCi kg^{-1} of ^{36}Cl (American Radiolabeled Chemicals, Inc. St. Louis, USA) and allowed to recover for 12 h. Fish were temporarily anesthetised (1ml of ethyl-*P*-amino-benzoate, 2.4 X 10^{-4} mol l^{-1} (Sigma, St Louis, MO, USA) in 2 L of water) and their vents were sutured shut and glued to eliminate urinary excretion for 7 h (the fish were too small to be fitted with urinary catheters). The fish were placed in their chambers and after 3 h water flow was stopped and 10 ml samples were collected for 4 h at hourly intervals to determine the appearance of ^{36}Cl. After 4 h, the fish were euthanized with benzocaine (ethyl-*P*-amino-benzoate, 2.4 X 10^{-4} mol l^{-1}, Sigma, St Louis, MO, USA) and blood samples (~300 μl) were collected by caudal puncture into heparinised syringes. Plasma was obtained by centrifugation (14 000 g for 3 min) and immediately frozen in liquid N_2. Plasma Cl^- levels were determined using a spectrophotometric method (Zall et al., 1956) modified for microplate, while Na^+, K^+ and Ca^{2+} concentrations were measured using an atomic

absorption spectrometer (AA240 Varian Inc., Mississauga, Canada). ^{36}Cl activity (converted from counts per minute (CPM) to disintegrations per minute (DPM) after quench correction) was measured by liquid scintillation counting (LS 6500 Multi-Purpose Scintillation Counter; Beckman Coulter, USA) using 4 ml of water mixed with 15 ml of scintillation cocktail (Bio-Safe II, Research Products International Corp, Illinois, USA) or 100 µl of plasma added to 3.9 ml of distilled water and 15 ml of scintillation cocktail. The average rate of appearance of ^{36}Cl in the water was determined from the slope of the linear regressions relating time and ^{36}Cl activity. $J_{OUT}Cl^-$ (in µmol kg^{-1} h^{-1}) was calculated according to the following formula:

$J_{OUT}Cl^-$ = [Δwater ^{36}Cl (DPM h^{-1})/plasma ^{36}Cl specific activity (DPM μmol^{-1})]/fish mass (kg).

To determine Cl^- influx ($J_{IN}Cl^-$), 0.5 µCi of ^{36}Cl was added to the aerated water and allowed to mix for 15 min. Water samples (10 ml) were taken hourly for 4 h and assessed for ^{36}Cl activity (see above) to obtain an average rate of ^{36}Cl disappearance. For these experiments, the vent was not sutured. $J_{IN}Cl^-$ (in µmol kg^{-1} h^{-1}) was calculated according to the following formula:

$J_{IN}Cl^-$ = [Δwater ^{36}Cl (DPM h^{-1})/water ^{36}Cl specific activity (DPM μmol^{-1})]/fish mass (kg).

Gill paracellular permeability

To assess the effect of temperature change and the associated changes in functional surface area on the paracellular permeability of the gills, fish were anesthetised and injected intraperitoneally with 50 µCi kg^{-1} of the extracellular marker ^{3}H-PEG 4000

(^{3}H-polyethylene glycol 4000; Perkin Elmer, USA) using an injection volume of 1.25 ml kg^{-1}. All other aspects of this experimental protocol were identical to the Cl^- efflux experiment previously described. Preliminary experiments (N = 6) comparing fish with and without sutured vents demonstrated that PEG efflux was reduced by 94% after suturing the vent. Thus, it is likely that this technique provides a reliable index of branchial PEG efflux.

Data presentation and statistical analysis

Data are presented as means ± 1 standard error of the mean (SEM). SigmaStat (version 3.0, SPSS Inc., Chicago, IL, USA) was used to perform statistical analysis. All data were evaluated by unpaired Student's t-test. In all cases, significance was set at $P < 0.05$.

Results

There were obvious differences in gill morphology in the fish acclimated to different temperatures. In fish that were acclimated to warm (25° C) water, the area of ILCM was significantly decreased when compared to the cold (7° C) acclimated fish (Fig. 2-1A). The surface area of the ILCM (expressed as a percentage of total interlamellar area) was 94.7 ± 1.4 in fish acclimated to 7° C (N = 6) and 28.3 ± 0.9 in fish maintained at 25° C (N = 6). Although not quantified in the present study, the reduction of the area of the ILCM resulted in an obvious increase in functional lamellar surface area (SA) in the warm water fish (compare Figs. 2-1B and 2-1C). In contrast to predictions, the reduction in the extent of the ILCM (and the associated increase in the functional SA of the gills) at 25° C was NOT accompanied by a significant increase in the total SA of ionocytes. Indeed, based on mitochondrial staining (Fig. 2-2, O_SO_4-ZnI_2 staining), the total ionocyte SA was markedly reduced in the fish kept at 25° C (2103 ± 180 compared to 5219 ± 438 μm^2 mm^{-1} of filament; Fig. 2-2A). The differences in total ionocyte SA at the two temperatures reflected differences in both the density of ionocytes and their individual sizes (Table 2-1). The ionocytes, while situated along the interlamellar regions and lamellar surfaces in the fish acclimated to 25° C, were confined largely to the outer edge of, or within, the ILCM in the fish acclimated to 7° C (Fig. 2-2B, C). Similar results were obtained when comparing the SA of ionocytes on the basis Na^+/K^+-ATPase (NKA) enrichment. The total SA of the NKA positive cells (Fig. 2-3A) was significantly lower in the warm water fish (1584 ± 170 μm^2 mm^{-1}) in comparison to the cold water fish (4146 ± 415 mm^2 mm^{-1}). The lower NKA positive cell SA at 25° C

was the result of lower frequency and smaller individual sizes (Table 2-1). At 7° C, the NKA positive cells were situated predominantly along the outer edge of the ILCM. The greater SA of the NKA positive cells in the fish acclimated to 7° C was not matched by an increase in branchial NKA activity; indeed NKA activity was markedly greater in the warm water fish (Fig. 2-4A) that exhibited fewer and smaller ionocytes. It is note worthy to remind that measurements for both conditions were done at room temperature. There was no statistically significant difference in the relative expression of branchial NKA mRNA between the two groups of fish (Fig. 2-4B); in part a consequence of large variability in the data.

To determine whether the appearance of ionocytes along the edge of the ILCM in the fish acclimated to 7° C was the result of migration of existing cells or differentiation of new cells, a time-differential double fluorescent staining technique was employed. The results demonstrated that the majority of the ionocytes appearing on the ILCM after a reduction in temperature had migrated from pre-existing cells [i.e. most of the cells were stained both red (^{TM}Mitotracker) and green (NKA positive)]. Additionally, however, a few new ionocytes appeared within the ILCM as indicated by the singly green-labeled cells in Figure 2-5. In comparison to the control fish kept at 7° C for 2 weeks, there were significantly greater numbers of newly formed ionocytes in fish transferred from 25° C to 7° C (27.5 versus 3.5% of total; Fig. 2-5A).

The effects of acclimation temperature on unidirectional Cl^- fluxes are depicted in Fig. 2-6. Although there were no statistically significant differences in the data, there were obvious trends for reduced rates of $J_{OUT}Cl^-$ (Fig. 2-6A) and $J_{IN}Cl^-$ (Fig. 2-6B). The data for $J_{NET}Cl^-$ (calculated on the basis of Cl^- concentration differences during flux

periods) were highly variable and also indicated no significant differences between the fish acclimated to 7° C (36.4 ± 74.0 μmol kg^{-1} h^{-1}; N = 6) or 25° C (-54.4 ± 12.6 μmol kg^{-1} h^{-1} N = 6). Net Cl^- fluxes calculated from the mean data (preventing statistical evaluation) of the unidirectional fluxes were -258 and -433 μmol kg^{-1} h^{-1} at 7 and 25° C, respectively. The levels of plasma Cl^- in the two groups of fish were consistent with the trends in the Cl^- flux data; plasma [Cl^-] was significantly lower in the fish acclimated to 25° C (70.5 ± 6.5 mmol l^{-1}) in comparison to the fish at 7° C (85.8 ± 6.9 mmol l^{-1}). Similarly, plasma [K^+] was significantly lower in the warmer fish whereas plasma [Na^+] and [Ca^{2+}] were hihger in fish acclimated to 25° C (Table 2-2).

Efflux of the extracellular marker PEG, an index of branchial paracellular permeability, was significantly greater (by approximately 7-fold) in the fish acclimated to warmer water (Fig. 2-7).

Figure 2-1. Mean data and representative micrographs illustrating the effects of acclimation temperature on relative interlamellar cell mass (ILCM) surface area in gills of goldfish (*Carassius auratus*). (A) The surface area of the ILCM (expressed as a percentage of total interlamellar area) was decreased (indicated by asterisk) in fish acclimated to 25° C (N = 6) when compared to fish kept at 7° C (N = 6); data are presented as means ± 1 SEM. (B, C) Representative light micrographs illustrate the marked differences in the extent of the ILCM (single ILCM's outlined in black) in the two groups of fish as well as the obvious increase in functional lamellar surface area in fish acclimated to 25° C; scale bars: 20 μm. The ionocytes are stained black.

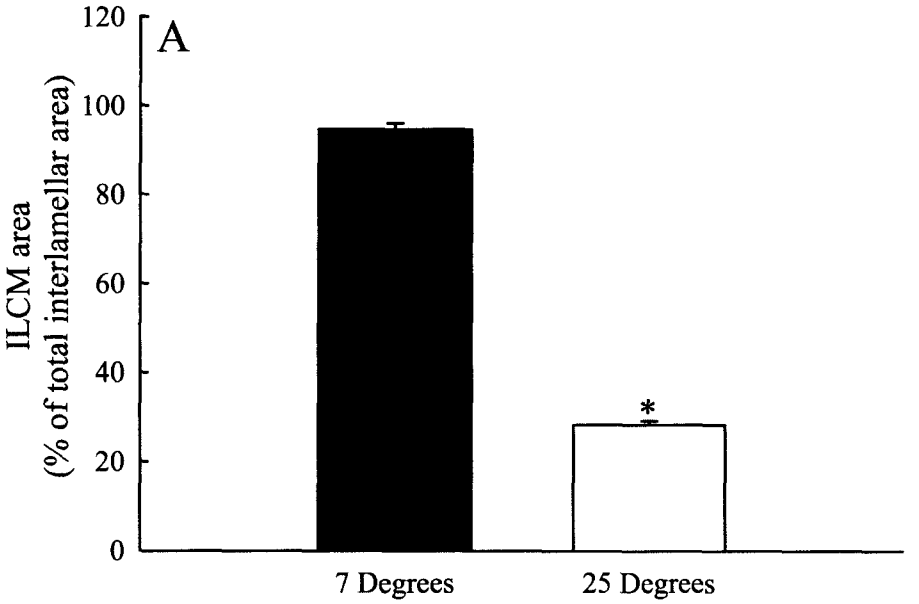
A
120
100
80
60
40
20
0
ILCM area
(% of total interlamellar area)
*
7 Degrees
25 Degrees

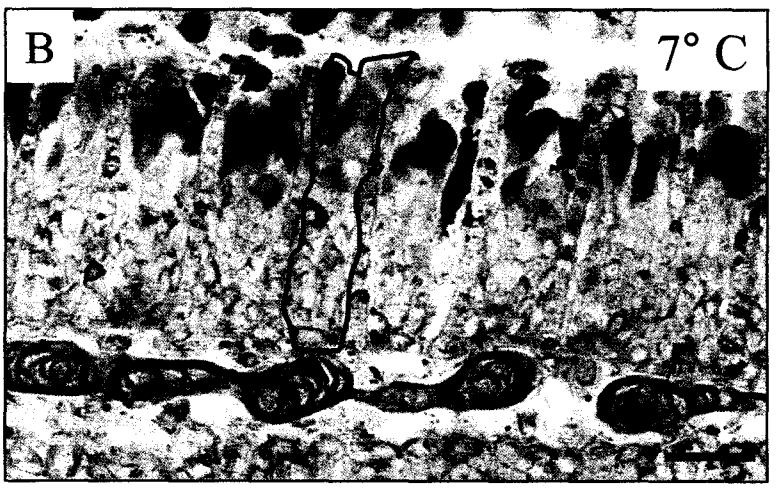
B
7° C

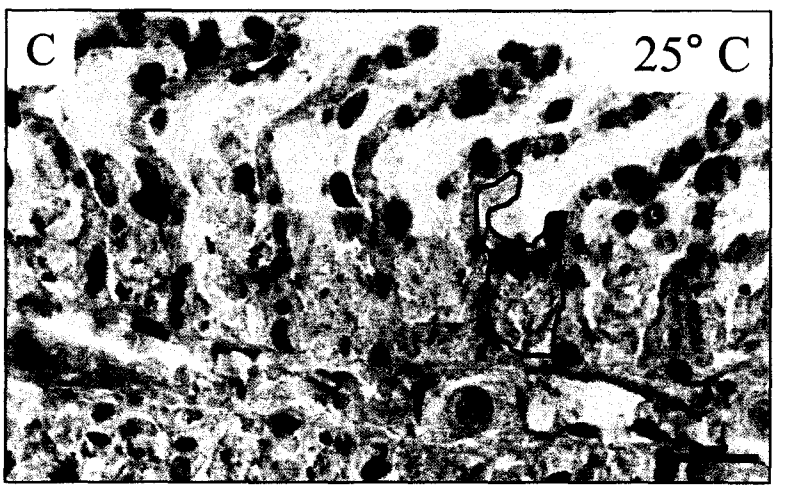
C
25° C

Figure 2-2. Mean data and representative micrographs illustrating the effects of acclimation temperature on the surface area of ionocytes (as determined using osmium-zinc iodide staining) and their distribution in goldfish (*Carassius auratus*). (A) The surface area of ionocytes (arrows) was significantly decreased (indicated by asterisk) in fish acclimated to 25° C (N = 6) when compared to fish kept at 7° C (N = 6); data are presented as means ± 1 SEM. (B, C) Representative light micrographs illustrate that the decrease in ionocyte surface area in fish acclimated to 25° C was a result of decreased numbers and sizes of individual cells (see Table 2-1). Note that the ionocytes were confined to the outer edge of the ILCM in the fish acclimated to 7° C; scale bars: 20 μm.

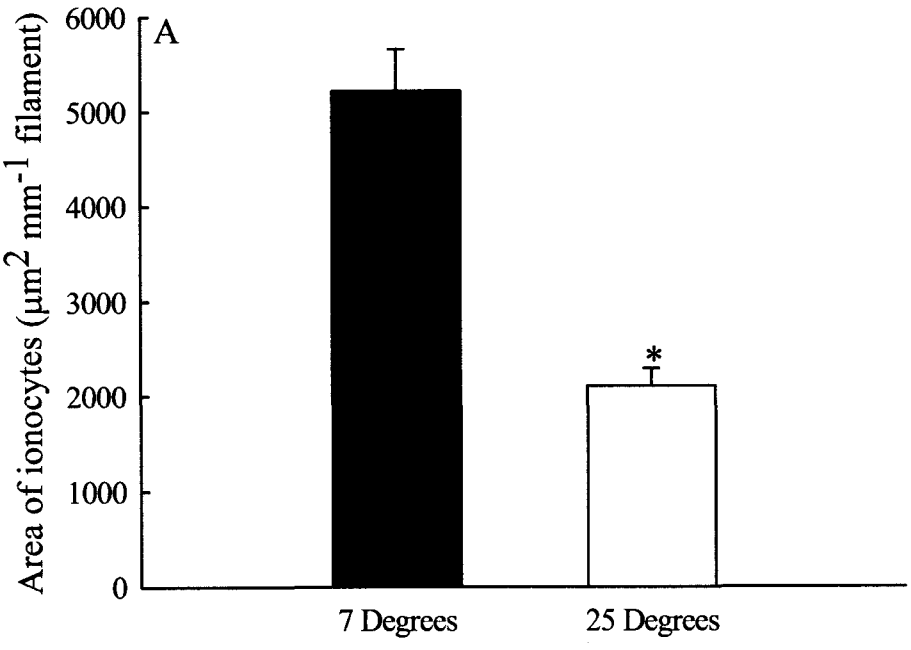
A
6000
5000
4000
3000
2000
1000
0
Area of ionocytes (μm2 mm-1 filament)
*
7 Degrees
25 Degrees

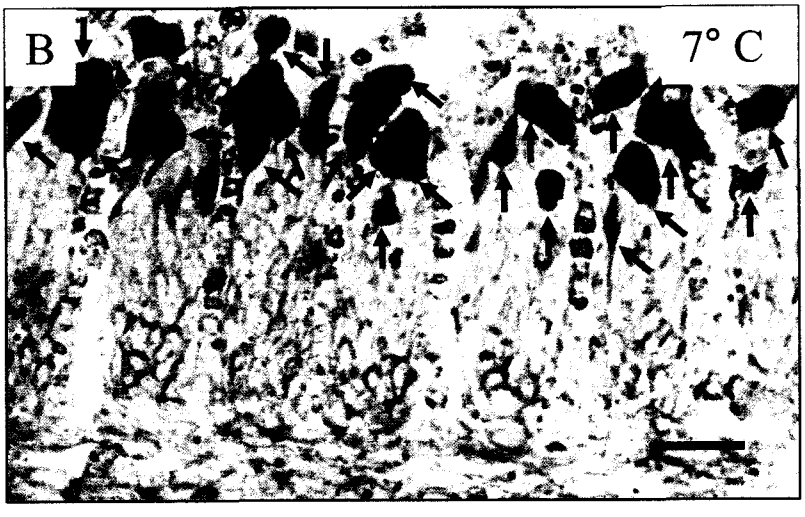
B
7° C

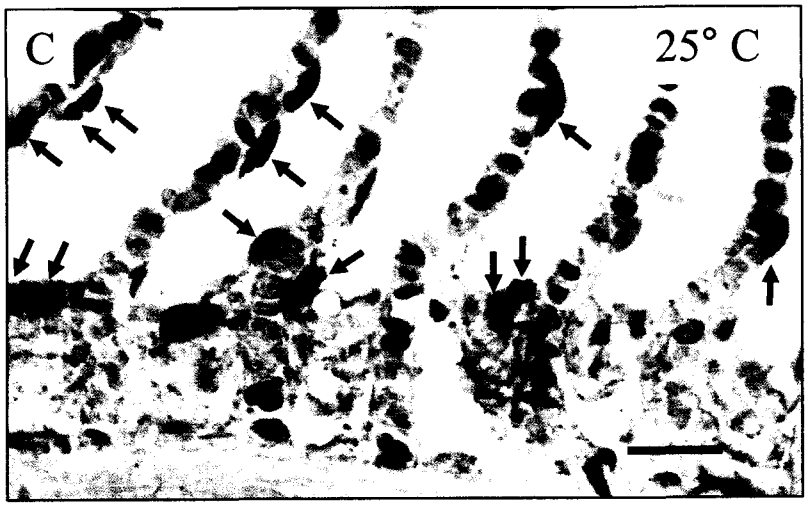
C
25° C

Figure 2-3. Mean data and representative micrographs illustrating the effects of acclimation temperature on the surface area of ionocytes (as determined by Na^+/K^+-ATPase immunofluorescence) and their distribution in goldfish (*Carassius auratus*). (A) The surface area of ionocytes (arrows) was significantly decreased (indicated by asterisk) in fish acclimated to 25° C (N = 6) when compared to fish kept at 7° C (N = 6); data are presented as means ± 1 SEM. (B, C) Representative light micrographs illustrate that the decrease in ionocyte surface area in fish acclimated to 25° C was a result of decreased numbers and sizes of individual cells (see Table 2-1). Note that the ionocytes were confined to the outer edge of the ILCM in the fish acclimated to 7° C; scale bars: 20 μm. Sections were labeled with DAPI-containing mounting media to show cell nuclei (blue).

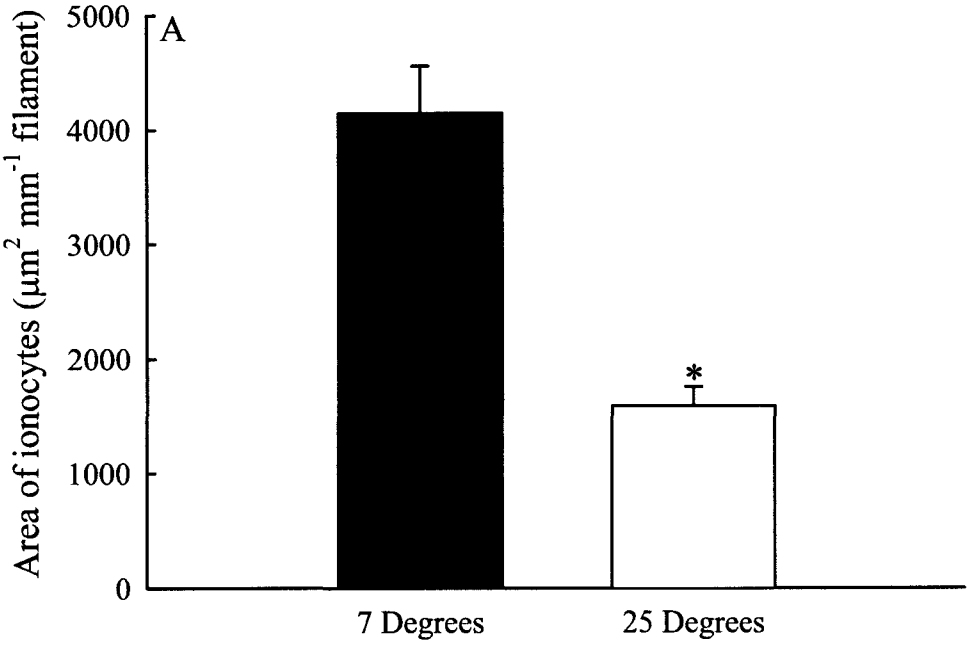
A
5000
4000
3000
2000
1000
0
Area of ionocytes (μm² mm⁻¹ filament)
*
7 Degrees
25 Degrees

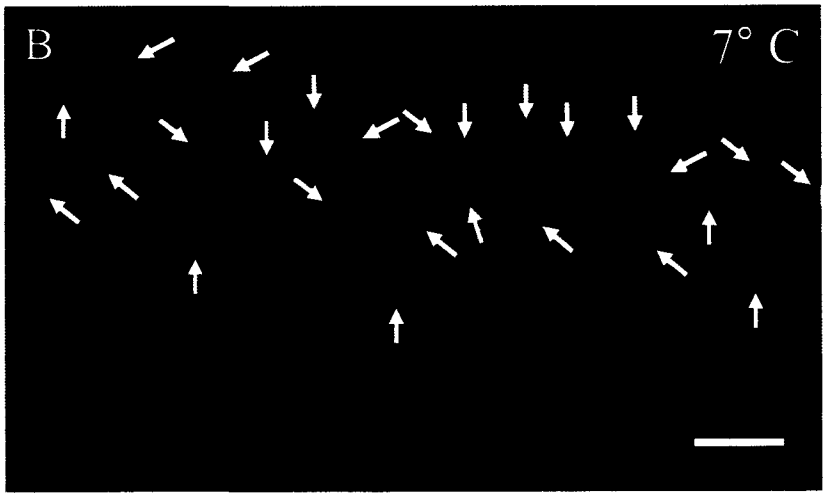
B
7° C

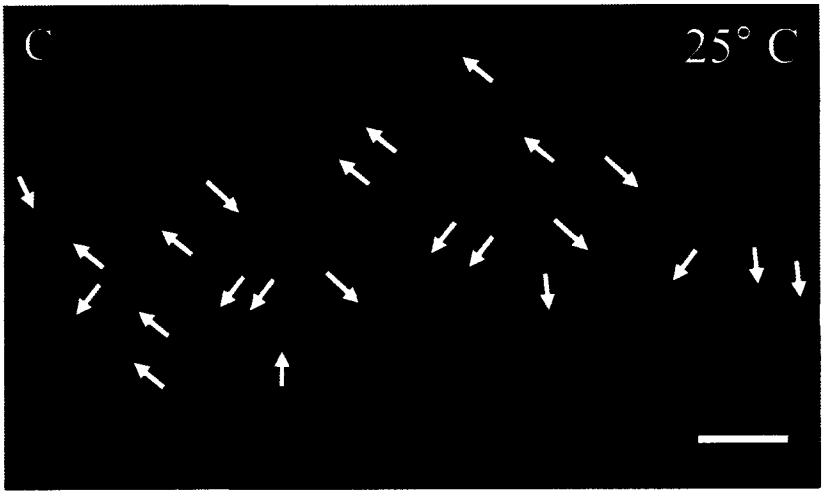
C
25° C

Figure 2-4. The effects of acclimation temperature on (A) branchial Na^+/K^+-ATPase (NKA) activity and (B) relative NKA mRNA levels in goldfish (*Carassius auratus*). (A) Branchial NKA activity was increased (indicated by asterisk) in fish acclimated to 25° C (N = 6) when compared to fish acclimated to7° C (N = 6). The expression of NKA mRNA in the fish acclimated to 25° C (N = 6) was not significantly increased (P = 0.065) when compared to fish at 7° C (N = 6) assigned a relative value of 1. Data are presented as means ± 1 SEM.

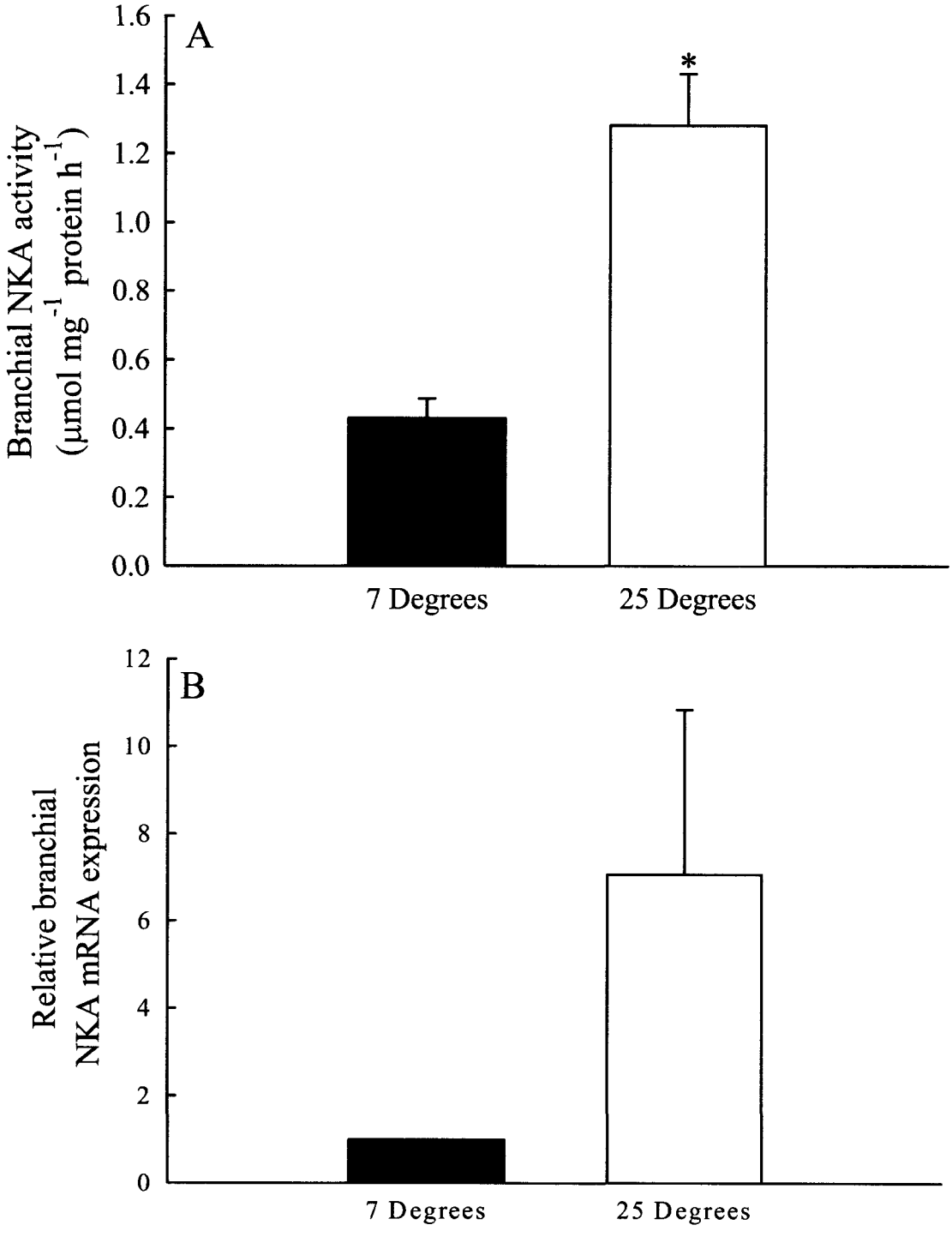
A
Branchial NKA activity
(μmol mg-1 protein h-1)
1.6
1.4
1.2
1.0
0.8
0.6
0.4
0.2
0.0
*
7 Degrees
25 Degrees
B
Relative branchial
NKA mRNA expression
12
10
8
6
4
2
0
7 Degrees
25 Degrees

Figure 2-5. The effects of decreasing temperature on the re-distribution of branchial ionocytes. Live fish were bathed in ^{TM}Mitotracker red and over the period of 2 weeks the temperature was brought down from 25° C to 7° C (N = 6); the gills were fixed, sectioned and incubated with α5 antibody (green) to localize Na^+/K^+-ATPase positive ionocytes. Thus, after 2 weeks, pre-existing ionocytes would either be single labeled red or doubled labeled red and green, while newly formed ionocytes would be single labeled and appear green only.

(A) The lowering of ambient temperature from 25° C to 7° C resulted in a significant increase (indicated by asterisk) in the number of newly formed ionocytes (unfilled portions of bars) while the number of pre-existing ionocytes was also increased (filled portions of bars) when compared to fish maintained at 7° C. Data are presented as means ± 1 SEM.

(B, C) After 2 weeks, proliferation of the interlamellar cell mass appeared to be accompanied by the migration of pre-existing ionocytes. Scale bar: 20 μm; cells were labeled with DAPI mounting media to show cell nuclei (blue).

(D, E) Newly formed ionocytes (arrows) were appearing in the ILCM. Scale bar: 20 μm; cells were labeled with DAPI mounting media to show cell nuclei (blue).

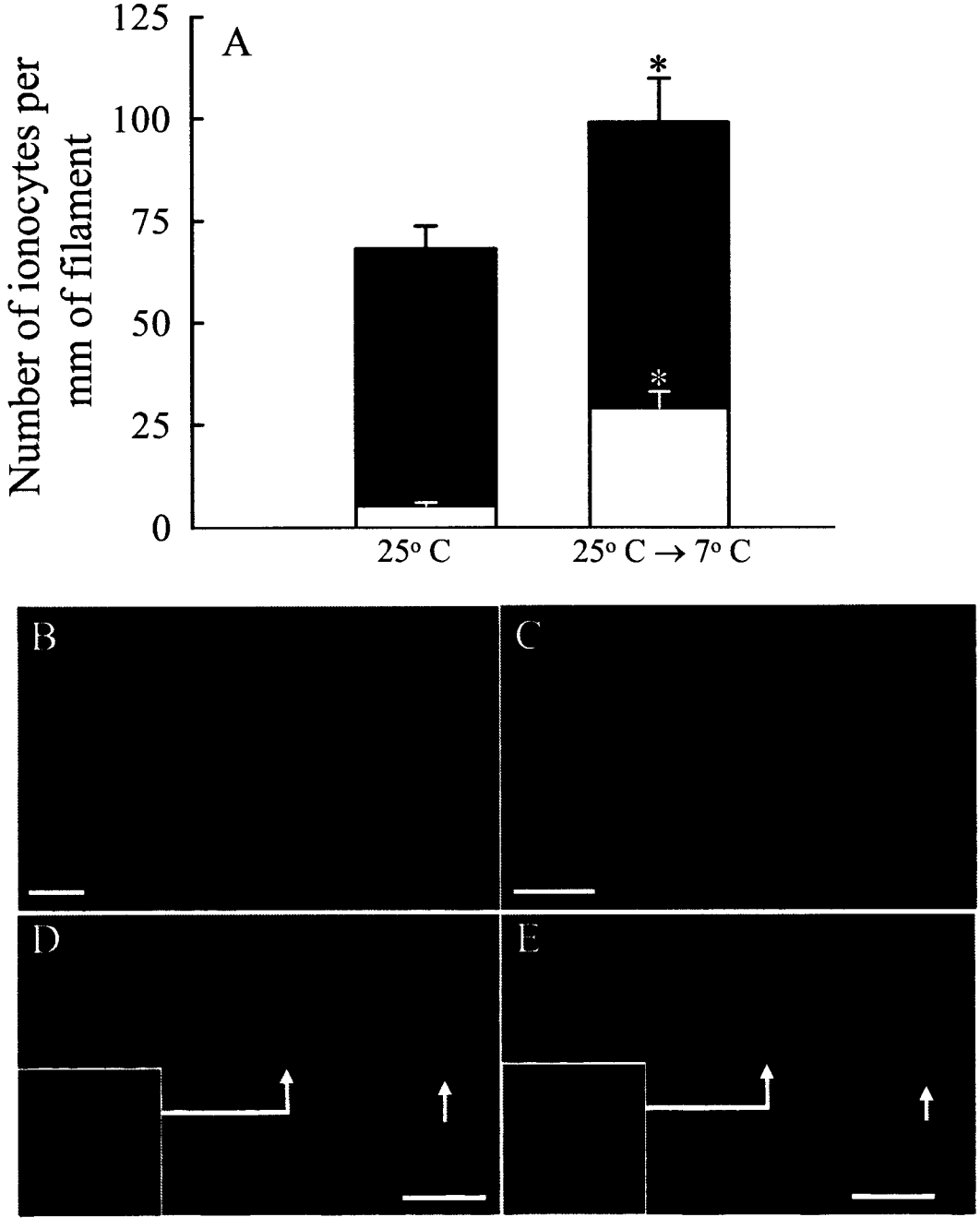
A
125
100
75
50
25
0
Number of ionocytes per mm of filament
*
*
25° C
25° C → 7° C
B
C
D
E

Figure 2-6. The effects of acclimation temperature on (A) branchial Cl^- efflux ($J_{OUT}Cl^-$; N = 6 for each temperature) and (B) whole body Cl^- influx ($J_{IN}Cl^-$; N = 6 for each temperature) in goldfish, *Carassius auratus*. There were no statistically significant differences between the two groups of fish; data are shown as means ± 1 SEM.

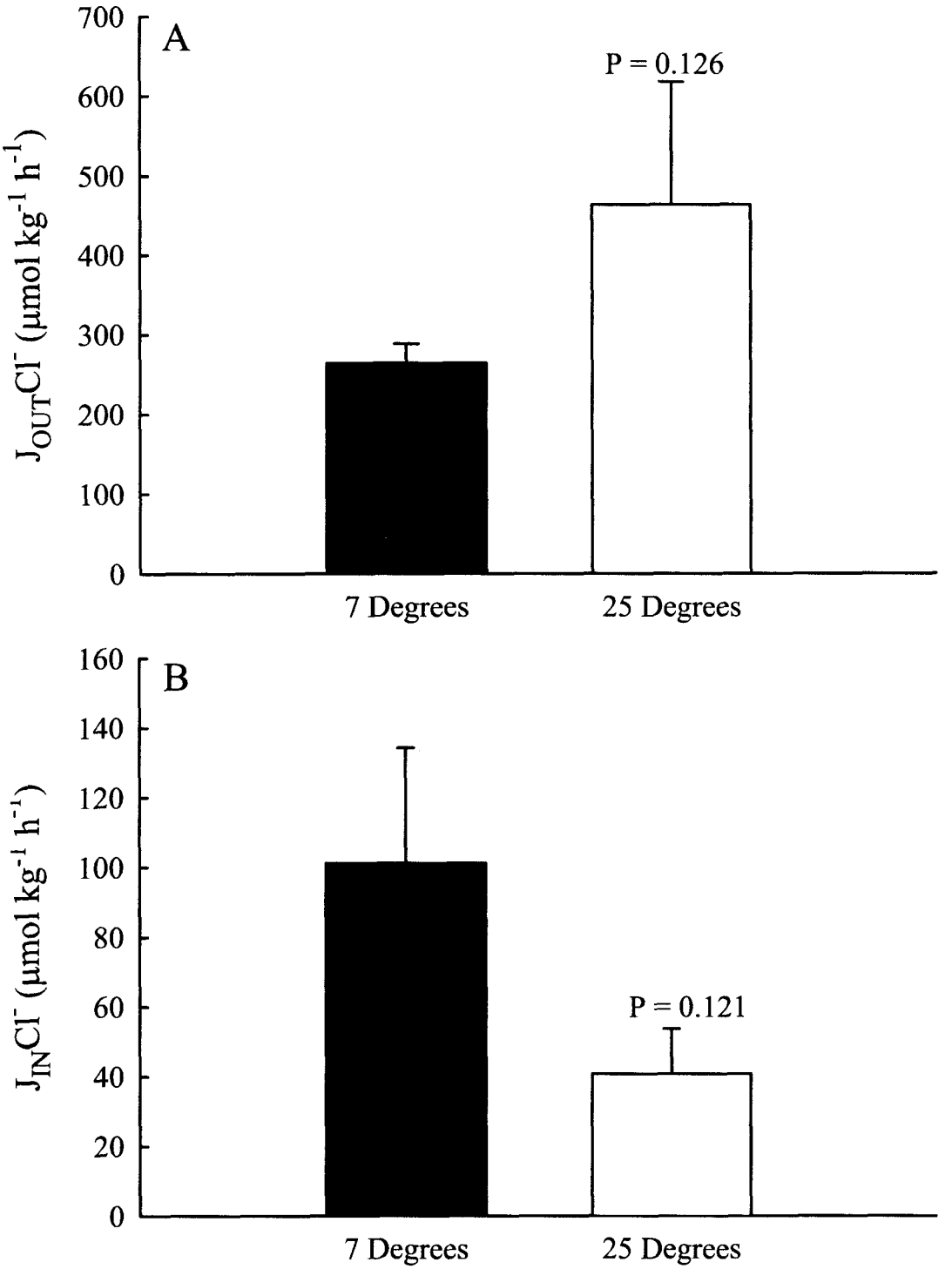
A
P = 0.126
700
600
500
400
300
200
100
0
$J_{OUT}Cl^-$ (μmol kg^{-1} h^{-1})
7 Degrees
25 Degrees
B
P = 0.121
160
140
120
100
80
60
40
20
0
$J_{IN}Cl^-$ (μmol kg^{-1} h^{-1})
7 Degrees
25 Degrees

Figure 2-7. The effects of acclimation temperature on branchial efflux of polyethylene glycol (PEG-4000) in goldfish, *Carassius auratus.* Data are presented as means ± 1 SEM.; a significant difference from 7° C is indicated by the asterisk.

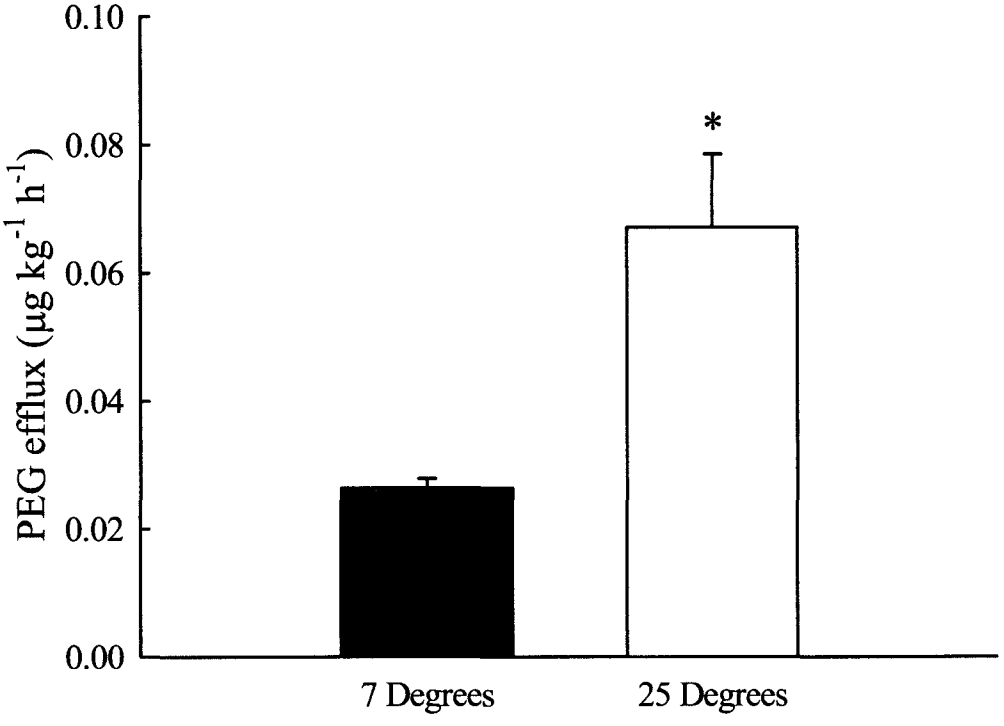
0.10
0.08
0.06
0.04
0.02
0.00
PEG efflux (µg kg-1 h-1)
*
7 Degrees
25 Degrees

Table 2-1. The effects of increased acclimation temperature on the numbers and two-dimensional surface areas of individual ionocytes as identified either using osmium-zinc iodide staining or Na^+/K^+-ATPase (NKA) immunofluorescence in goldfish (*Carassius auratus*). Data are presented as means ± SEM. Significant differences from values at 7° C are indicated by asterisks ($P < 0.05$; $N = 6$ for both groups).

		7° C	**25° C**
Osmium-zinc iodide technique	Average ionocyte surface area (μm^2)	53.2 ± 4.7	*37.0 ± 2.8
	Average number of ionocytes per mm of filament	101.1 ± 3.2	*58.0 ± 5.4
NKA immunofluorescence technique	Average ionocyte surface area (μm^2)	42.1 ± 4.9	*25.1 ± 3.3
	Average number of ionocytes per mm of filament	96.6 ± 5.2	*67.1 ± 10.6

Table 2-2. The effect of increased acclimation temperature on plasma ion levels in goldfish (*Carassius auratus*). Data are presented as means ± 1 SEM. Significant differences from values at 7° C are indicated by asterisks ($P < 0.05$; N = 11 for both groups).

	7° C (N = 11)	**25° C (N = 11)**
$[Cl^-]$ (mmol l^{-1})	85.8 ± 6.9	*70.5 ± 6.5
$[Na^+]$ (mmol l^{-1})	103.5 ± 3.5	*131.2 ± 8.1
$[K^+]$ (mmol l^{-1})	6.6 ± 0.5	*5.1 ± 0.4
$[Ca^{2+}]$ (mmol l^{-1})	5.8 ± 1.05	*10.9 ± 1.1

Discussion

The major findings of this study are that i) branchial ionocytes remain largely exposed to the water regardless of the presence or absence of an ILCM, ii) the perpetual exposure of ionocytes to the water reflects the migration of pre-existing cells and differentiation of progenitor cells, iii) the ion transporting capacity of the gill (as estimated by ionocyte SA) was not enhanced in fish exhibiting an increase in functional lamellar surface area but instead was markedly reduced, and iv) fish appeared to specifically regulate branchial Cl^- loss in the face of increasing functional lamellar surface area despite a marked increase in general paracellular permeability (PEG efflux).

The distribution and putative functions of ionocytes in fish with or without an ILCM

In fish acclimated to 7^o C, the ionocytes were localized to the outer regions of, and to a lesser extent, within the ILCM whereas in fish lacking an ILCM, the ionocytes were distributed along the lamellar and filament epithelia. Thus, in each situation, the ionocytes are exposed to inspired water where they are presumed to be functional ion transporting cells. The relocation of ionocytes to outer regions of the ILCM in the cold-water acclimated fish is consistent with our hypothesis that ionic uptake would otherwise be severely constrained if lamellar or filament ionocytes were covered by the ILCM. On the other hand, the decrease in the surface area of ionocytes in the fish without an ILCM (and hence possessing a greater functional lamellar surface area) was not in accordance with the prediction that increased ion-transporting capacity is required in such instances to counteract increased passive loss of ions. It is puzzling that the changes in ionocyte

SA were not accompanied by similar changes in NKA activities and clearly this result begs the question as to which metric is a better indicator of branchial ion transport capacity. Given the tight correlation between ionocyte SA and ionic uptake in FW teleosts (Perry et al., 1992a; Perry et al., 1992b) and the reports of a lack of correspondence between NKA activities and ionocyte abundance (McCormick, 1995; Sloman et al., 2001), the more reliable indicator would seem to be ionocyte SA. The fact that Cl^- uptake did not correlate with ionocyte SA in the present study suggests that one or more other factors (including NKA activity) are regulating this process in the fish experiencing gill remodeling.

Regardless of the underlying explanation for the mismatch between ionocyte SA and NKA activities, the increase in NKA activity with temperature reported here is similar to the previous results of Murphy and Houston (1974) who demonstrated an approximate 2.5-fold greater branchial NKA activity in goldfish acclimated to 5 and 35° C.

As in other freshwater teleosts, branchial Cl^- uptake in goldfish is thought to occur via an apical membrane electroneutral Cl^-/HCO_3^- exchanger (Maetz and Garcia Romeu, 1964; Garcia Romeu and Maetz, 1964; De Renzis and Maetz, 1973; Preest et al., 2005). The specific genes responsible for Cl^-/HCO_3^- exchange in the fish gill have not been identified with certainty although members of the SLC4 and SLC26 gene families have been implicated by immunocytochemistry (Wilson et al., 2000; Piermarini et al., 2002). In current models of ionic regulation, the apical membrane Cl^-/HCO_3^- exchanger typically is localized to a subset of ionocytes that are believed to be functionally analogous to the base secreting (B-type) intercalated cells of the mammalian collecting duct (Perry et al.,

2003a; Perry et al., 2003b; Evans et al., 2005; Perry and Gilmour, 2006; Marshall and Grosell, 2006; Tresguerres et al., 2006; Claiborne et al., 2008). Another subset of ionocytes is thought to be analogous to the acid secreting (A-type) intercalated cells of the collecting duct in which an apical membrane Na^+/H^+ exchanger and/or Na^+ channel/VATPase linked process act to absorb Na^+ (Reid et al., 2003; Lin et al., 2006; Horng et al., 2007; Parks et al., 2007; Yan et al., 2007; Hwang and Lee, 2007). Phenotypically different populations of ionocytes have been identified in several fish species including rainbow trout [*Oncorhynchus mykiss* (Goss et al., 2001)], killifish [*Fundulus heteroclitus* (Laurent et al., 2006)], zebrafish [*Danio rerio* (Hwang and Lee, 2007)] and tilapia [*Oreochromis mossambicus* (Hiroi et al., 2008)]. Different sub-populations of ionocytes have not yet been identified in goldfish but it is conceivable that if existing, the lack of correlation between total ionocyte SA and Cl^- uptake in the fish undergoing gill remodeling may reflect a change in the relative abundance of ionocyte subtypes. For example, unaltered rates of Cl^- uptake in the fish exhibiting increased total ionocyte SA (fish acclimated to 7° C) might simply result from a preferential increase in ionocyte subtypes involved in other ion transport functions (e.g. Na^+ uptake). Another factor to consider when relating ionocyte SA to rates of Cl^- uptake is their placement within the gill. In fish acclimated to 25° C, the ionocytes are localized on lamellar and filament epithelia in close proximity to blood channels and capillaries, respectively, enabling efficient substrate removal and replenishment. In the fish acclimated to 7° C, the ionocytes are restricted to the edge of the ILCM which is thought to be devoid of a vascular supply (Sollid et al., 2003). Thus, one should expect that the uptake of Cl^- in the cold water fish would be constrained by the slow rate of its entry into the circulation.

Thus, it is conceivable that the proliferation of ionocytes in the fish acclimated to cold water is a response aimed at aiding ion uptake given their inhospitable location (at least with respect to blood flow). One can also speculate that the reduced blood supply and associated O_2 deprivation in the vicinity of the ionocytes also contribute to lowering the levels of NKA per cell which might explain the discrepancy between total ionocyte SA and NKA activities. Further studies should attempt to determine if the function of the ionocytes on the ILCM is constrained by inadequate perfusion.

Recently, Chou et al. (2008) demonstrated a pronounced proliferation of ionocytes in zebrafish acclimated to cold (12° C) water that coincided with increased mRNA expression of several branchial genes involved in ion uptake including the epithelial calcium channel and cytosolic carbonic anhydrase (CA2-like isoform). It was suggested that a global up-regulation of branchial genes involved in ionic and acid-base regulation was an appropriate response to mitigate the disruptive effects of cold temperature.

The contribution of cell migration versus cell differentiation in the redistribution of ionocytes during gill remodeling

Katoh and Kaneko (2003) described a novel method for establishing the relative contributions of cellular differentiation and transformation to ionocyte replacement in killifish transferred from sea water to fresh water. In the present study, we have adapted their "time-differential double fluorescent staining" technique to evaluate the dynamics of ionocyte redistribution associated with gill remodeling in goldfish transferred from 25 to 7° C. Our interest was to determine the relative importance of cell migration compared to

cell differentiation in the redistribution of ionocytes to the outer edge of the newly formed ILCM. The original method of Katoh and Kaneko (2003) used two fluorescent mitochondrial markers (^{TM}Mitotracker red and ^{TM}Mitotracker green) to distinguish pre-existing from newly formed ionocytes. While we were able to achieve suitable and persistent (2 weeks) staining by bathing live fish with ^{TM}Mitotracker red, we were less successful when using a second application of ^{TM}Mitotracker green two weeks later. Thus, we modified the original protocol of Katoh and Kaneko (2003) by using the α5 antibody (to localize NKA) on tissue sections derived from fish previously subjected to ^{TM}Mitotracker red (two weeks earlier). The interpretation of the data obtained using this double labeling technique relies on the assumption that ^{TM}Mitotracker and the NKA antibody are indeed labeling the same cell type. We believe that this is a reasonable assumption especially given the remarkably similar changes in ionocyte numbers and surface areas as determined using the two different techniques (Table 2-1). While all cells positive for NKA are likely to be enriched with mitochondria (and hence labeled with ^{TM}Mitotracker), there may be a sub-population of mitochondria enriched cells that are not enriched with NKA as observed for the V-ATPase enriched ionocytes of zebrafish (Hwang and Lee, 2007). Even if such cells exist in goldfish, the conclusions regarding cell migration and differentiation would not be altered given the likelihood that all NKA positive cells are also identified using ^{TM}Mitotracker.

The redistribution of ionocytes from filament to lamellar epithelia was previously described in rainbow trout during acclimation to ion-poor water (Laurent et al., 1995). It was concluded that the appearance of additional ionocytes on the lamellar epithelium in fish acclimated to ion-poor water largely reflected differentiation of filament stem cells

and their migration to lamellae. Because the migration of ionocytes from filament to lamella is thought to be relatively slow (e.g. 4 days; Chretien and Pisam, 1986), it was proposed that the rapid (as early as 12 h) appearance of lamellar ionocytes in the fish kept in ion-poor water may have resulted from differentiation of lamellar stem cells (Laurent et al., 1995) thought to reside in the inner layer of the multi-layered lamellar epithelium (Laurent, 1984). We do not know the origin of the newly formed ionocytes in the fish transferred from 25 to 7° C. Interestingly, the new ionocytes which accounted for about 30% of the total ionocyte population in fish acclimated to 7° C, were never found on the outer edge of the ILCM but instead tended to be located within the cell mass, itself.

Paracellular permeability and transepithelial Cl^- fluxes in fish with or without an ILCM

In accordance with theory, the large difference in functional lamellar surface area in the fish acclimated to 7 or 25° C resulted in a markedly increased branchial efflux of the paracellular flux marker PEG (Wood et al., 1998) in the warm water acclimated fish. Although not quantified in the present study, the extent of gill remodeling in goldfish acclimated to the two temperatures appeared qualitatively to be similar to the degree of gill remodeling observed in crucian carp exposed to hypoxia (Sollid et al., 2003). Because the increases in PEG efflux (7.5-fold) was equivalent to the increase in functional lamellar surface area (7.4-fold) observed in crucian carp during exposure to hypoxia (Sollid et al., 2003), it seems likely that branchial paracellular permeability to PEG was not altered by acclimation temperature and that the increase in efflux at higher temperature simply reflected the increased functional surface area. On the other hand, the paracellular efflux of Cl^- at higher temperature was constant and did not vary with the

presumed increase in surface area (7.4-fold). Thus, these results provide evidence for a specific regulation of Cl^- permeability as surface area increases so as to minimize the paracellular loss of Cl^-.

The rate and specificity of solute movement through paracellular pathways is thought to be governed by several families of proteins that comprise tight junctions (Anderson et al., 2004). The two most widely studied tight junction protein families are the claudins and occludin (Gonzalez-Mariscal et al., 2003). Recently, claudins or occludin have been identified in the gills of a variety of fish species where they have been implicated in regulating paracellular salt permeability during salinity transfer (Bagherie-Lachidan et al., 2008; Lundgreen et al., 2008; Tipsmark et al., 2008a; Tipsmark et al., 2008b; Tipsmark et al., 2008c) or ionic imbalance imposed by food deprivation (Chasiotis and Kelly, 2008). There is emerging evidence that specific claudin proteins can differentially regulate the paracellular movement to anions and cations. For example, over-expression of claudin-7 in cultured porcine kidney cells causes a decrease in paracellular Cl^- conductance while simultaneously increasing paracellular Na^+ conductance (Alexandre et al., 2005). It would be useful in future studies to determine the effects of gill remodeling on the relative expression of goldfish gill tight junction proteins.

Another factor presumably reducing the paracellular efflux of Cl^- in the warm water acclimated fish is a lowering of the blood-to-water diffusion gradient because plasma [Cl^-] was approximately 15 mmol l^{-1} lower (Table 2-2) in the fish at 25° C. Combined, lowering the Cl^- diffusion gradient and selective "tightening" of the paracellular pathways to Cl^-, provide an effective strategy to reduce the costs of

absorbing Cl^- in fish with increased functional surface area. Indeed, the rate of Cl^- uptake was not increased in the fish at 25° C suggesting no additional costs of transporting Cl^-. Although there were no statistically significant changes in Cl^- efflux or influx in the warm water fish when measured after two weeks of acclimation, there was an obvious net negative flux of Cl^- (at least when considering the mean data). Thus, it would appear that the measured levels of plasma Cl^- can only be maintained at steady state via supplementary dietary uptake of Cl^-.

CHAPTER 3

PHYSIOLOGICAL CONSEQUENCES OF GILL REMODELING IN GOLDFISH (*CARASSIUS AURATUS*) DURING EXPOSURE TO LONG-TERM HYPOXIA

Chapter 3 is based on a manuscript to be submitted to American Journal of Physiology

Mitrovic, D., Dymowska, A., Nilsson, G.E., and Perry, S.F. (2009). Physiological consequences of gill remodeling in goldfish (*Carassius auratus*) during exposure to long-term hypoxia *J.Exp.Biol.* In Press.

Abstract

Goldfish (*Carassius auratus*) acclimated to 7° C and exposed to hypoxia (~10 mm Hg) for 7 days exhibited a pronounced remodeling of the gill consisting of the retraction of an interlamellar cell mass (ILCM). Subsequent experiments were designed to assess the impact of gill remodeling and the associated increase in functional lamellar surface area on Cl^- balance. Despite the increased functional lamellar surface area during hypoxia, there was no corresponding increase in Cl^- loss or efflux of the extracellular marker polyethylene glycol (PEG). However, when hypoxic fish were returned to normoxic water for 12 h, rates of Cl^- and PEG efflux were markedly stimulated in keeping with an increased surface area for solute movement. Similarly, the rate of branchial Cl^- uptake was reduced (105 ± 22 *versus* 45 ± 8 μmol kg^{-1} h^{-1} in normoxic and hypoxic fish, respectively) but then markedly stimulated (345 μmol kg^{-1} h^{-1}) upon reestablishment of normoxic conditions. Hypoxia (7 days) was accompanied by a significant decrease in the surface area of branchial ionocytes owing to a decrease in their numbers and individual sizes; shorter periods (1 or 3 days) of hypoxia were without effect. Despite unchanging (1 and 3 days) or reduced (7 days) numbers of ionocytes, branchial Na^+/K^+-ATPase activity was increased in hypoxic fish. These data demonstrate that despite experiencing an increase in functional lamellar surface area, hypoxic goldfish limit branchial Cl^- loss likely by a hypoxia-mediated decrease in paracellular permeability, an energetically effective strategy that obviates the need to increase rates of Cl^- uptake. Regardless of water oxygen status, the ionocytes were largely confined to the outer edges of the ILCM. By using a "time differential double staining technique"

(Katoh and Kaneko, 2003), it was demonstrated that during hypoxia, pre-existing ionocytes migrated with the shrinking ILCM while a smaller proportion of newly differentiated cells appeared below the surface of the ILCM. The capacity to maintain a population of ionocytes in contact with the water is an appropriate strategy to retain ionoregulatory capabilities regardless of whether the lamellae are uncovered or covered.

Introduction

Many species of fish have adopted strategies to survive extended periods of hypoxia which may occur commonly in aquatic environments (Wu, 2002). Some hypoxia tolerant species, including crucian carp (*Carassius carassius*) and goldfish (*Carassius auratus*) can survive extended periods (months) of hypoxia in cold water (Bickler et al., 2000) by reducing metabolic rate and exploiting large glycogen stores to fuel anaerobic metabolism (Hyvarinen et al., 1985). While anaerobic metabolism may provide necessary energy for the fish, the duration of hypoxia tolerance is limited by the prevailing glycogen stores (Nilsson, 1990). Thus, it is clearly advantageous for such animals to postpone for as long as possible the switch from aerobic to anaerobic metabolism (Nilsson and Renshaw, 2004). In crucian carp, this is accomplished by maintaining a low functional surface area of the gill under normoxic conditions and by remodeling the gill during exposure to hypoxia to increase functional surface area (Nilsson, 2007; Sollid and Nilsson, 2006; Sollid et al., 2003; Sollid et al., 2005). The remodeling of the gill in hypoxic crucian carp involves the retraction of an interlamellar cell mass (ILCM) causing the exposure of previously covered lamellar surfaces (Sollid et al., 2003). Although increasing surface area will benefit O_2 uptake, it is likely to hinder osmotic and ionic regulation owing to increased rates of passive salt loss and water uptake (Gonzalez and McDonald, 1992; Randall et al., 1972). Thus, the energetic costs associated with osmoregulation will be increased in freshwater (FW) owing to the need to increase the active (ATP-dependent) absorption of salts. The trade off between the need to maximize functional surface area for gas transfer and the benefit of a reduced surface

area to limit the costs of osmoregulation is termed the osmorespiratory compromise (Randall et al., 1972). Thus, the crucian carp utilizes an effective strategy to reduce metabolic expenditures by dynamically linking gill functional surface area with gas transfer requirements.

Goldfish, like crucian carp, exhibit gill remodeling when exposed to cold ambient temperatures. Specifically, Sollid et al. (2005) demonstrated that acclimatization of goldfish to 7° C resulted in a marked decrease in gill functional surface area owing to the formation of an ILCM. Although no data currently exist, it is reasonable to expect that like crucian carp, goldfish exposed to severe hypoxia at 7° C would increase gill functional surface area by retraction of the ILCM. If occurring, such an increase in functional surface area might cause an increase in passive ion loss that would need to be matched by an increase in the capacity for active ion uptake to prevent ionic imbalance. In the present study, we have focused on the consequences of hypoxia induced gill remodeling on Cl^- uptake. The cells believed to be responsible for Cl^- uptake in FW fish are the mitochondrion rich cells (MRC) or FW chloride cells (Perry, 1997; Perry et al., 2003; Tresguerres et al., 2006). Because there are numerous subtypes of fish MRC that may transport different ions, use of the term "ionocyte" is gaining favour to denote generically all members of the MRC family (Hwang and Lee, 2007). Thus, in this study, we hypothesize that the increased passive efflux of Cl^- that is presumed to accompany the elevated gill functional surface area in hypoxic goldfish will be matched by equivalent increases in Cl^- uptake owing to an increase in the numbers of ionocytes. In fish without an ILCM, the ionocytes are typically found in greatest abundance on the filament epithelium within the interlamellar channels and on basal regions of the lamellar

epithelium. Thus, to ensure that Cl^- uptake capacity is maintained in fish with or without an ILCM, we predict that the ionocytes will be positioned so as to always remain in contact with the water. Therefore, in normoxic fish at 7^o C, we speculate that the ionocytes will largely be confined to the outer regions of the ILCM whereas in hypoxic fish, the ionocytes will migrate with the retracting ILCM so as to remain exposed to the external environment.

Materials and Methods

Experimental animals

Goldfish, *Carassius auratus* (23.9 ± 0.4 g, N = 207; Along's International, Mississauga, Canada), were acquired and held for at least one week in circular tanks provided with dechlorinated city of Ottawa tap water at 18° C. After the initial acclimation period, the water temperature was decreased daily by 2° C to reach a final acclimation temperature of 7° C. Fish were maintained under a 12h: 12h light: dark photoperiod and were fed once a day with commercial food pellets. The fish were maintained at 7° C for at least two weeks prior to their use in any experiments. Twenty four h prior to the onset of the experiments, fish were moved to individual boxes (approximately 600 ml) that were supplied with flowing aerated water at acclimation temperature. Once in these individual chambers, fish were exposed to hypoxic (see below) or normoxic conditions and were not fed.

Hypoxia was achieved by gassing a water equilibration column supplying the fish with N_2 to maintain PO_2 at 6% of air saturation (~10 mm Hg); the duration of hypoxia was either 1, 3 or 7 days. In some experiments, hypoxic fish were returned to normoxic water and allowed to recover for 1 or 2 weeks. The experiments were concluded by killing the fish by anesthetic overdose (benzocaine; ethyl-P-amino-benzoate, 2.4 X 10^{-4} mol l^{-1}, Sigma, St Louis, MO, USA); gill tissues or blood and water samples were taken for further analysis. All experiments using live animals were performed according to institutional guidelines in accordance with the Canadian Council on Animal Care (CCAC).

Light microscopy and immunocytochemistry

Upon removal of the gill arches, filaments from arches 1 and 2 (left side) were placed into a solution of zinc iodide-2% osmium tetroxide (3:1 ratio) for at least 24 h at room temperature (Garcia-Romeu and Masoni, 1970). The samples were then cryo-protected using 15% sucrose (12 h) followed by 30% sucrose. All samples were stored in 30% sucrose at 4° C prior to use. The gills were embedded in OCT cryosectioning medium (VWR), incubated for 20 min and sectioned horizontally (10 μm sections) using a cryostat (Leica CM 1850 Laboratories Eq., Germany). Sections were placed on microscopy slides (Superfrost Plus; Fisher) and mounted with 60% glycerol under a cover slip.

For immunocytochemistry, gill filaments from arches 1 and 2 (right side) were placed directly into 4% paraformaldehyde and left overnight at 4° C. Tissues were cryo-protected in sucrose and sectioned (10 μm thick sections) using a cryostat (see above). Sections were placed on microscopy slides (Superfrost Plus; Fisher) and allowed to incubate for 1 h at room temperature prior to being stored at 4°C until required. Following 3 X 5 min washes with PBST (0.1M phosphate buffered saline, 0.3% Triton-X 100) and blocking with sheep serum (1:10 dilution, Sigma) for 1 h, sections were incubated for 2 h at room temperature with primary antibody: α5 (1:100), a mouse monoclonal antibody against the α1 sub-unit of chicken Na^+/K^+-ATPase (University of Iowa Hybridoma Bank). The α5 antibody has been used successfully for immunocytochemistry in numerous vertebrate species including fish (e.g. Wilson et al., 2000). For negative controls, sections were incubated with 1X PBST buffer lacking primary antibody. Immunofluorescence was detected after incubating the sections with a

1:400 dilution of Alexa Fluor-546 coupled to goat anti-mouse IgG (Fisher, Ottawa, ON, Canada) for 1 h. After washing (3 x 10 min in 0.1X PBS), sections were mounted in Vectashield mounting medium (Vector Labs, Canada) and cover slipped.

For each fish, 2 gill sections were examined using light or epifluorescence microscopy. Photos (4 per fish) from "randomly" selected areas of the mid regions of the gill filament were taken at 40X magnification. Photos were taken using an Axiophot (Zeiss, Germany) microscope, Olympus DP70 digital microscope camera and Image Pro Plus software Version 6.0 (Media Cybernetics Inc., Bethesda, USA). Digital images were analyzed using web-based imaging software (Image J, Waine Rasband, Maryland, USA) to determine morphological variables including numbers and surface areas of ionocytes (stained black using zing iodide – osmium tetroxide or exhibiting enrichment of NKA by immunofluorescence) and the relative surface area of the ILCM.

Na^+/K^+ ATPase activity

The third gill arch from each fish was added to SEI buffer (150 mmol l^{-1} sucrose, 10 mmol l^{-1} EDTA, 50 mmol l^{-1}imidazole), frozen in liquid N_2 and stored at -80° C. Na^+/K^+ ATPase activity was determined (in triplicate) in the supernatant of homogenized samples using a spectrophotometric microplate assay according to McCormick (1993). Ouabain-sensitive ATPase activity was measured and expressed in units of μmoles ADP mg^{-1} protein h^{-1} and compared to ATPase activity in the absence of ouabain. Protein was determined using the bichinchonic acid method (BIORAD) according to the instructions of the manufacturer.

"Time-differential double fluorescent staining" of ionocytes

To determine whether ionocytes were migrating with the ILCM during hypoxia exposure or alternatively appearing as newly differentiated ionocytes, the "time-differential double fluorescent staining" technique of Katoh and Kaneko (2003) was adopted with the following modifications. Only one ^{TM}MitoTracker (MitoTracker Red CMXRos, Molecular Probes) was used; fish were exposed to this fluorescent mitochondria-specific dye for 4 h (1 μmol l^{-1}) in normoxic water. Fish were then exposed to running hypoxic water for 7 days; control fish were maintained in normoxic water. After the duration of hypoxia, fish were euthanized (see above) and gill tissue was removed, fixed and sectioned for immunocytochemistry as described previously while allowing as little exposure to light as possible. To detect NKA-enriched cells, the α5 monoclonal antibody was used in conjunction with the secondary antibody Alexa Fluor-488 (green) coupled to goat anti-mouse IgG (Fisher, Ottawa, ON, Canada). Because we previously demonstrated that all NKA-enriched cells in goldfish will stain positively with ^{TM}MitoTracker (unpublished observations), this protocol allows time-dependent differential labeling of the ionocytes. Thus, if a cell is stained both red and green (positive for both ^{TM}Mitotracker and NKA), it existed prior to the onset of hypoxia exposure whereas if a cell is stained only green (^{TM}MitoTracker negative, NKA positive), it is assumed that this is a new ionocyte that did not exist at the beginning of the experiment.

Real-time RT-PCR Total RNA was extracted from 100 mg of gill tissue using TRIzol Reagent (Invitrogen) and re-suspended in 40 μl of nuclease-free water. Reverse

transcription was performed using the Revertaid H Minus M-MuLV reverse transcriptase enzyme according to the protocol for cDNA synthesis provided by the manufacturer (Fermentas, Life Sciences). The following modifications were made: the final reaction volume was 20 µl and 2 µl of RNA was used with 0.2 µg or random hexamer primers. An MX 3000 Multiplex Quantitative PCR System (Stratagene) and Brilliant SYBR Green QPCR Master Mix (Stratagene) were used for the real-time RT-PCR as per the instructions of the manufacturer with slight modifications: the total reaction volume was adjusted to 12.5 µl, 1 µl of cDNA template was used and final primer concentrations were 100 nmol l^{-1}. Annealing and extension temperatures were 55° C (1 min) and 72° C (1min) for over 40 cycles. All the primers used for real time PCR (including the reference gene 18S ribosomal RNA) were designed using web-based software (primer3; http://frodo.wi.mit.edu/cgi-bin/primer3/primer3_www.cgi). To obtain homologous primers to amplify goldfish NKA, a 485 bp nucleotide sequence obtained from a BLAST search of GenBank (Accession FG392680) was used to provide a product size of 123 bp.

NKA 1α (09a01);

Forward primer 5'-CGAGGTACCGTCACCATTCT-3',

Reverse primer 5'-GTCTGTTTTGGGGTTTCTGG-3'

Primers for 18S ribosomal RNA were designed from a 551 bp nucleotide sequence obtained from a BLAST search of GenBank (Accession AF047349);

Forward primer 5'-GAGCCTGAGAAACGGCTACC-3',

Reverse primer 5'-CCATGGGTTTAGATATGCTC-3'

The specificity of the primers was verified by cloning and sequencing of the amplified products. To ensure that residual genomic DNA was not being amplified,

control experiments were performed in which reverse transcriptase was omitted during cDNA synthesis. Relative expression of mRNA levels was determined (using 18S RNA as an endogenous standard) by a modification of the Δ-Δ Ct method (Pfaffl, 2001). Amplification efficiencies were determined from standard curves generated by serial dilution of plasmid DNA.

Chloride fluxes and plasma analysis

To assess the effects of hypoxia exposure and gill remodeling on Cl^- efflux ($J_{OUT}Cl^-$), fish were lightly anesthetized and injected intraperitoneally with 40 μCi kg^{-1} of ^{36}Cl (American Radiolabeled Chemicals, Inc. St. Louis, USA) and allowed to recover for 12 h. Fish were temporarily anesthetized (1ml of ethyl-*P*-amino-benzoate, 2.4 X 10^{-4} mol l^{-1} (Sigma, St Louis, MO, USA) in 2 L of water) and their vents were sutured shut and glued to eliminate urinary excretion for 7 h (the fish were too small to be fitted with urinary catheters). The fish were placed in their chambers and after 3 h water flow was stopped and 10 ml samples were collected for 4 h at hourly intervals to determine the appearance of ^{36}Cl. After 4 h, the fish were euthanized with benzocaine (ethyl-*P*-amino-benzoate, 2.4 X 10^{-4} mol l^{-1}, Sigma, St Louis, MO, USA) and blood samples (~300 μl) were collected by caudal puncture into heparinised syringes. Plasma was obtained by centrifugation (14 000 g for 3 min) and immediately frozen in liquid N_2. Plasma Cl^- levels were determined using a spectrophotometric method (Zall et al., 1956) modified for microplate, while Na^+, K^+ and Ca^{2+} concentrations were measured using an atomic absorption spectrometer (AA240 Varian Inc., Mississauga, Canada). ^{36}Cl activity (converted from counts per minute (CPM) to disintegrations per minute (DPM) after

quench correction) was measured by liquid scintillation counting (LS 6500 Multi-Purpose Scintillation Counter; Beckman Coulter, USA) using 4 ml of water mixed with 15 ml of scintillation cocktail (Bio-Safe II, Research Products International Corp, Illinois, USA) or 100 μl of plasma added to 3.9 ml of distilled water and 15 ml of scintillation cocktail. The average rate of appearance of ^{36}Cl in the water was determined from the slope of the linear regressions relating time and ^{36}Cl activity. $J_{OUT}Cl^-$ (in μmol kg^{-1} h^{-1}) was calculated according to the following formula:

$J_{OUT}Cl^-$ = [Δwater ^{36}Cl (DPM h^{-1})/plasma ^{36}Cl specific activity (DPM μmol^{-1})]/fish mass (kg).

To determine Cl^- influx ($J_{IN}Cl^-$), 0.5 μCi of ^{36}Cl was added to the aerated water and allowed to mix for 15 min. Water samples (10 ml) were taken hourly for 4 h and assessed for ^{36}Cl activity (see above) to obtain an average rate or ^{36}Cl disappearance. For these experiments, the vent was not sutured. $J_{IN}Cl^-$ (in μmol kg^{-1} h^{-1}) was calculated according to the following formula:

$J_{IN}Cl^-$ = [Δwater ^{36}Cl (DPM h^{-1})/water ^{36}Cl specific activity (DPM μmol^{-1})]/fish mass (kg).

Gill paracellular permeability

To assess the effect of hypoxia and the associated changes in functional surface area on the paracellular permeability of the gills, fish were anesthetized (as above) and injected intraperitoneally with 50 μCi kg^{-1} of the extracellular marker ^3H-PEG 4000 (^3H-polyethylene glycol 4000; Perkin Elmer, USA) using an injection volume of 1.25 ml kg^{-1}. All other aspects of this experimental protocol were identical to the Cl^- efflux experiment

previously described. Preliminary experiments (N = 6) comparing fish with and without sutured vents demonstrated that PEG efflux was reduced by 94% after suturing the vent. Thus, it is likely that this technique provides a reliable index of branchial PEG efflux.

Data presentations and statistical analysis

Statistical analysis was performed using Sigma Stat (version 3.0, SPSS Inc, Chicago, IL, USA). Numerical data are presented as means ± of SEM (standard error of the mean). Statistical significance for all data sets were evaluated using 1-way or 2-way ANOVA, except for changes in gill NKA mRNA expression which were analyzed using one-sample Student's *t*-tests. Significance of all data results was set at $P< 0.05$.

Results

There were marked time-dependent changes in the morphology of the gill ILCM in fish exposed to hypoxia (~10 mm Hg). The area of the ILCM (expressed as a percentage of total interlamellar area) varied between 90.5 and 96.8 in fish maintained at 7° C in normoxic water (Fig. 3-1A). Exposure of fish to hypoxia for 1 day caused a reduction of the ILCM area to 69.4 ± 1.0%; after 7 days the area of the ILCM was reduced to only 39.1 ± 1.8% of the total interlamellar area (Fig. 3-1A). Re-exposure of hypoxic fish to normoxia caused a reappearance of the ILCM that was complete after 2 weeks (Fig. 3-1A). Although not quantified in the present study, the reduction of the ILCM during hypoxia was associated with an increase in lamellar functional surface area (SA) (e.g. compare Figs. 3-1B and 3-1C).

The effects of 7 days of hypoxia on unidirectional Cl^- fluxes (as measured both under hypoxic and normoxic conditions) are depicted in Fig. 3-2. When measured under the prevailing hypoxic conditions, there was no significant difference in $J_{OUT}Cl^-$ in fish previously exposed to hypoxia for 7 days. However, when assayed under normoxic conditions, there was a pronounced increase in $J_{OUT}Cl^-$ in the fish acclimated to hypoxia (Fig. 3-2A). $J_{IN}Cl^-$ was reduced in hypoxic fish (Fig. 2B); however, the hypoxia exposed fish exhibited a marked increase in $J_{IN}Cl^-$ when assayed under normoxic conditions (Fig. 3-2B). The data for $J_{NET}Cl^-$ (calculated on the basis of Cl^- concentration differences during flux periods) were highly variable and indicated no significant differences between the fish acclimated to hypoxia for 7 days and the normoxic fish. Net Cl^- fluxes calculated from the mean data (preventing statistical evaluation) suggested that hypoxic

fish were experiencing a greater net loss of Cl^- (-20 and -131 μmol kg^{-1} h^{-1} in the normoxic and hypoxic fish, respectively). Returning the hypoxic fish to normoxic water caused an increase in $J_{NET}Cl^-$ to 60 μmol kg^{-1} h^{-1}. The levels of plasma Cl^- in the two groups of fish were consistent with the trends in the Cl^- flux data; plasma [Cl^-] was significantly reduced in the fish acclimated to 7 days of hypoxia (67.7 ± 3.8 mmol l^{-1}) in comparison to the normoxic fish (93.9 ± 5.8 $mmol^{-1}$).

Efflux of the extracellular marker PEG, an index of branchial paracellular permeability, was significantly reduced (by approximately 3-fold) in the fish acclimated to (and assessed in) hypoxic water (Fig. 3-3A). When assessed under normoxic conditions, PEG efflux was markedly enhanced (by approximately 2-fold) in the fish previously acclimated to hypoxia (Fig. 3-3B).

The total SA of ionocytes (deduced as the product of cell size (area) and cell numbers) was decreased in hypoxic fish (Fig. 3-4A; Table 3-2). In normoxic fish, total ionocyte area averaged about 5000 μm^2 per mm of filament length (Fig. 3-4A). After 7 days of hypoxia, total ionocyte area was decreased to 2890 ± 141 μm^2 mm^{-1} (Fig 3-4A) owing exclusively to a reduction in their numbers (Table 3-2). In normoxic fish, the ionocytes were largely confined to the outer edge of the ILCM whereas in hypoxic fish, the ionocytes were situated predominantly within the interlamellar regions and along lamellar surfaces (Fig. 3-4B, C). Similar results were obtained when comparing the SA of ionocytes on the basis of Na^+/K^+-ATPase (NKA) enrichment. The SA of NKA positive cells (Fig. 3-5A) was significantly lowered in the fish exposed to 7 days of hypoxia (2702 ± 165 μm^2 mm^{-1}) in comparison to the normoxic fish (4535 ± 320 μm^2 mm^{-1}). The decrease in the SA of NKA positive cells during hypoxia was the result of a

reduction in their frequency; the size of individual NKA positive cells was unchanged in fish exposed to hypoxia for 7 days (Table 3-2). The decreases in the SA of the NKA positive cells were no longer apparent in the 2 week recovery group. Similar to the ionocytes identified using zinc iodide staining, the NKA positive cells were situated predominantly along the outer edge of the ILCM in normoxic fish whereas in hypoxic fish, the ionocytes were largely localised within the interlamellar regions and along lamellar surfaces (Fig. 3-5). The decrease in the SA of the NKA positive cells in the fish acclimated to hypoxia was not matched at the functional level by a decrease in branchial NKA activity; indeed, enzyme activity was increased from 1 - 7 days of hypoxia and persisted at least until 7 days of recovery in normoxic water (Fig. 3-6A). The relative expression of branchial mRNA for NKA was increased after 7 days of hypoxia (Fig. 3-4B).

To determine whether the relocation of ionocytes during retraction of the ILCM in hypoxic fish was a result of migration of existing ionocytes and/or differentiation of new ionocytes, a "time-differential double fluorescent staining technique" was employed. The results demonstrated (Fig. 3-7) that the majority of the relocated cells had migrated from pre-existing cells [i.e. most of the cells were stained both red (^{TM}Mitotracker) and green (NKA positive)]. Additionally, however, a few new ionocytes appeared within the ILCM as indicated by singly green-labeled cells (Fig. 3-7B, C). In comparison to control fish kept in aerated water for 2 weeks, there were significantly greater numbers of newly formed ionocytes in fish exposed to 7 days of hypoxia (17.2% *versus* 4.9% of total; Fig. 3-7A).

Figure 3-1. Mean data and representative micrographs illustrating the effects of acclimation to hypoxia and subsequent normoxic recovery on relative interlamellar cell mass (ILCM) surface area in gills of goldfish (*Carassius auratus*). (A) The surface area of the ILCM (expressed as a percentage of total interlamellar area) was decreased (indicated by asterisks) in fish after only 1 day in hypoxic water and returned to control levels after two weeks of recovery under normoxic conditions. Data are presented as means ± 1 SEM; N = 6 for all groups. (B, C) Representative light micrographs illustrate the marked differences in the extent of the ILCM (representative single ILCM's outlined in black) in the normoxic and hypoxic fish as well as the obvious increase in functional lamellar surface area in fish acclimated to hypoxia; scale bars: 20 μm; the ionocytes are stained black.

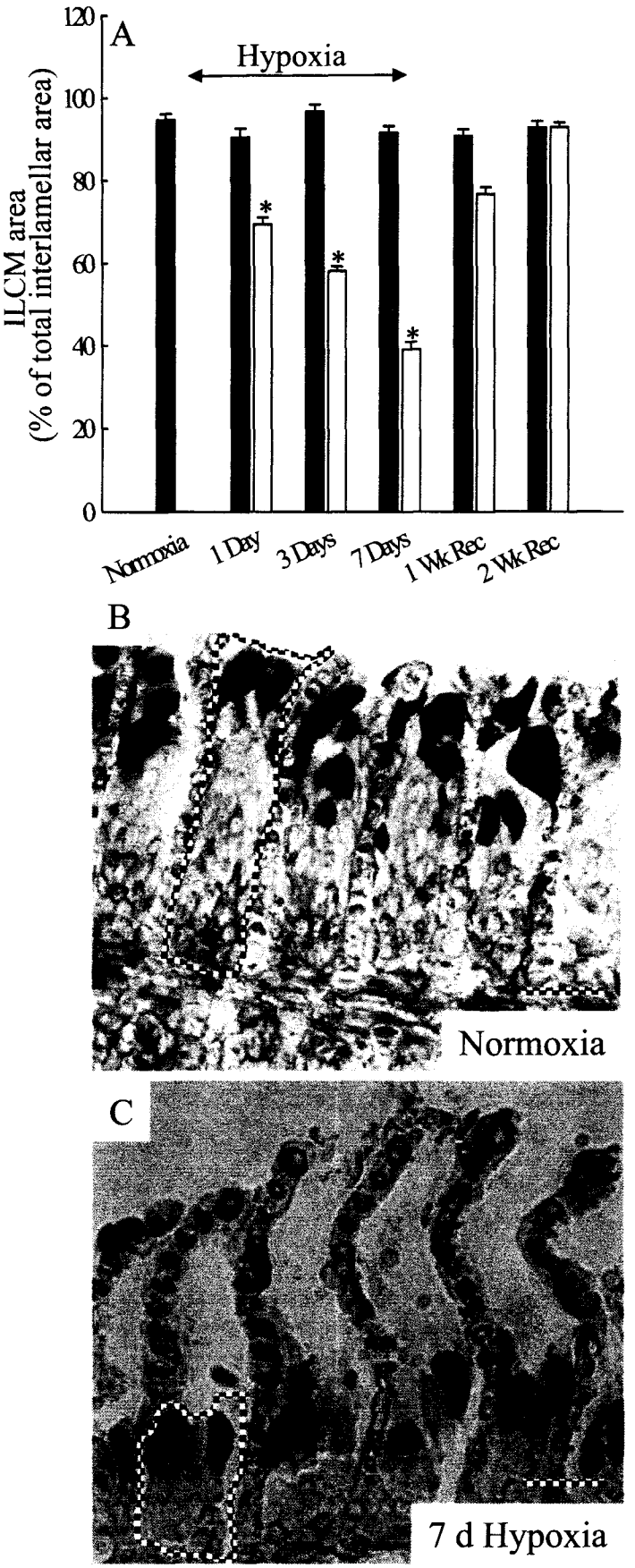
A
Hypoxia
ILCM area
(% of total interlamellar area)
120
100
80
60
40
20
0
*
*
*
Normoxia
1 Day
3 Days
7 Days
1 Wk Rec
2 Wk Rec
B
Normoxia
C
7 d Hypoxia

Figure 3-2. The effects of exposure to hypoxia for 7 days on (A) branchial Cl^- efflux ($J_{OUT}Cl^-$; N = 6 for all groups) and (B) whole body Cl^- influx ($J_{IN}Cl^-$; N = 6 for all groups) in goldfish, *Carassius auratus*. In one set of experiments (hypoxia), fluxes were conducted under prevailing acclimation conditions (normoxia = filled bars; hypoxia = unfilled bars) while in another set of experiments (hypoxia → normoxia), fluxes were conducted under normoxic conditions only. Data are presented as means ± 1 SEM; values not sharing a common letter are statistically different ($P < 0.05$).

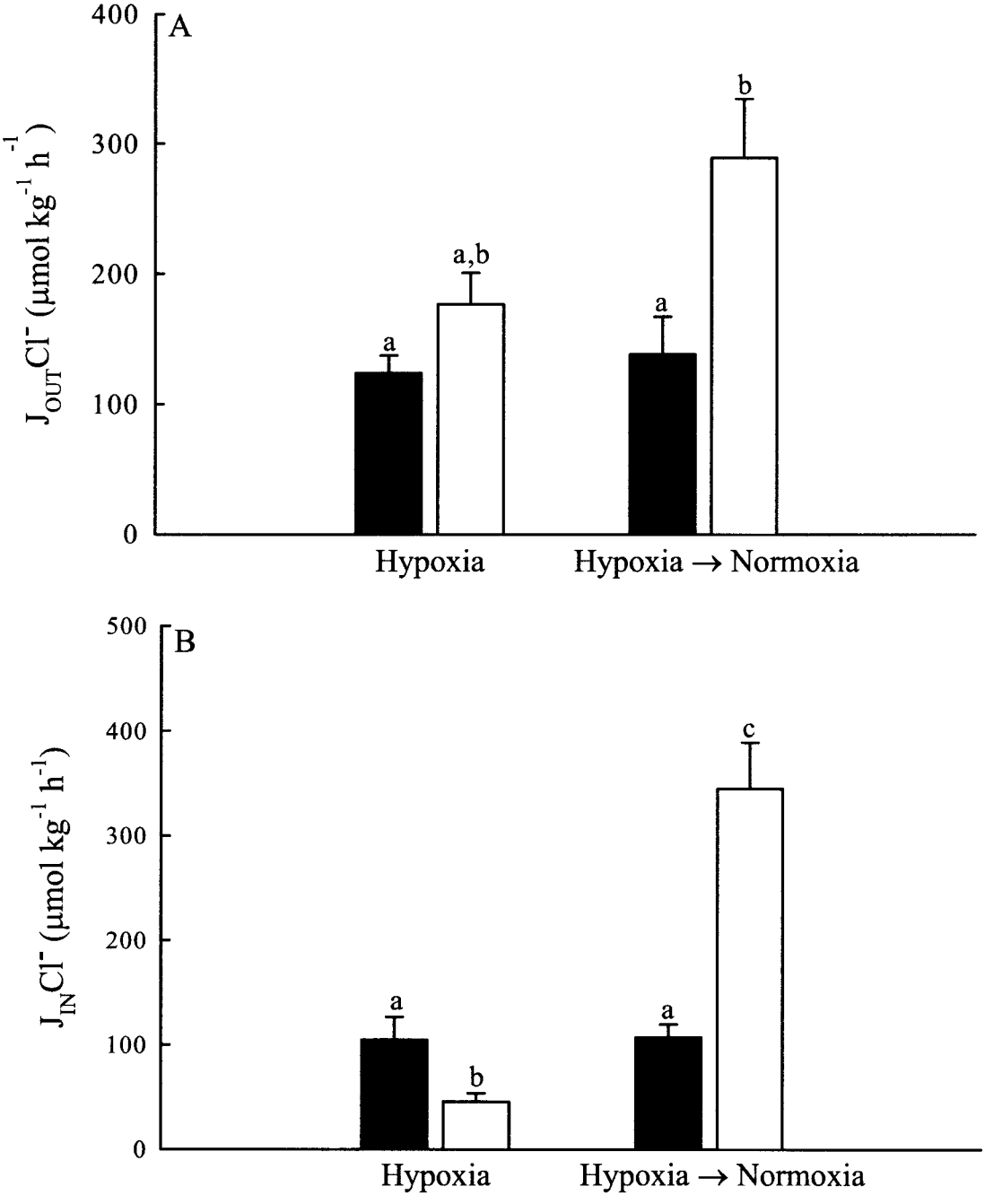
A
400
300
200
100
0
$J_{OUT}Cl^-$ (µmol kg^{-1} h^{-1})
a
a,b
a
b
Hypoxia
Hypoxia → Normoxia
B
500
400
300
200
100
0
$J_{IN}Cl^-$ (µmol kg^{-1} h^{-1})
a
b
a
c
Hypoxia
Hypoxia → Normoxia

Figure 3-3. The effects of exposure to hypoxia on branchial efflux of polyethylene glycol (PEG) as determined under (A) prevailing acclimation conditions (normoxia = filled bars; N = 5; hypoxia = unfilled bars; N = 5) or (B) normoxic conditions (N = 6 for each group). Data are presented as means ± 1 SEM; significant differences from values in fish acclimated to normoxia are indicated by asterisks ($P < 0.05$).

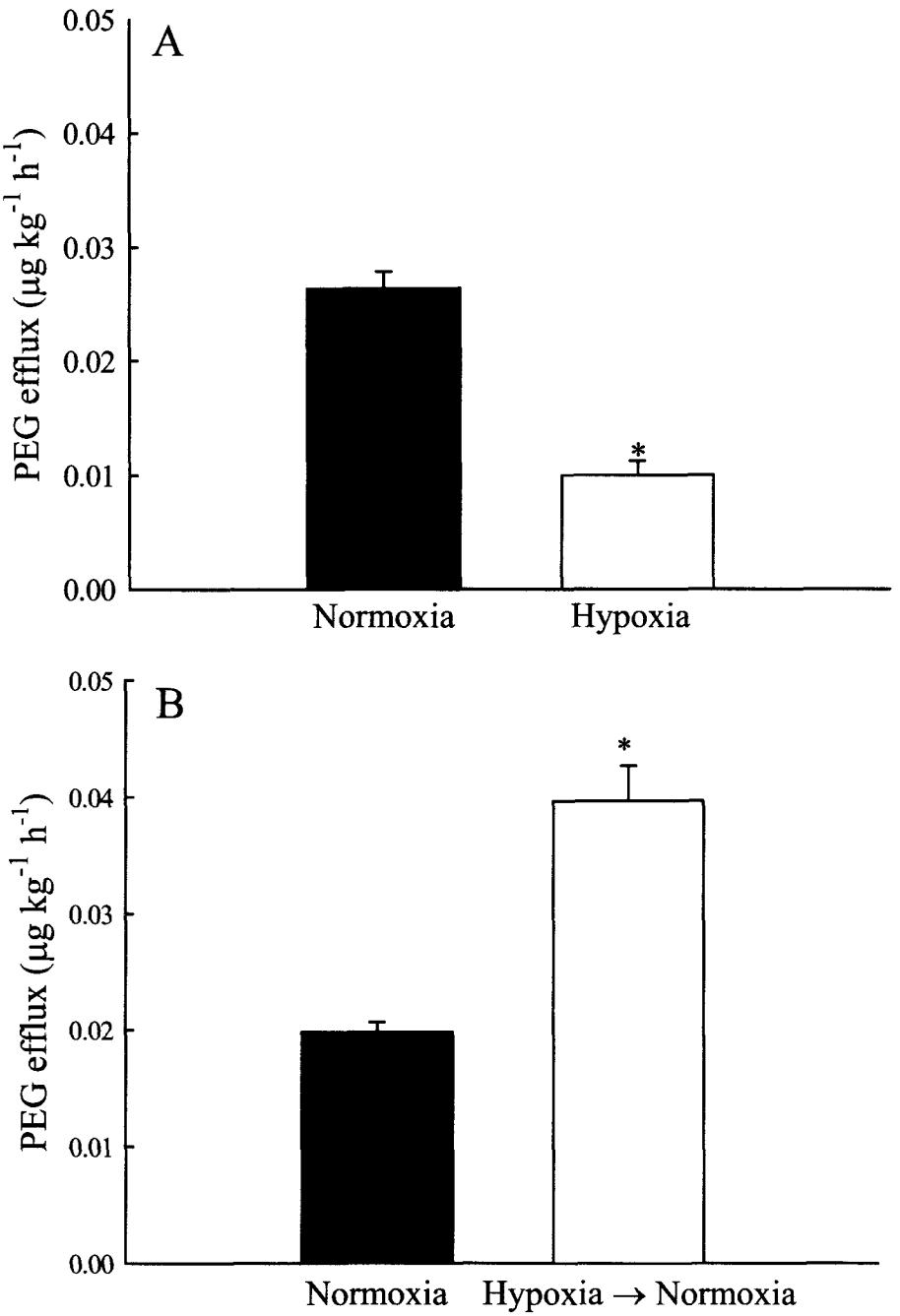
A
0.05
0.04
0.03
0.02
0.01
0.00
PEG efflux (μg kg-1 h-1)
*
Normoxia
Hypoxia
B
0.05
0.04
0.03
0.02
0.01
0.00
PEG efflux (μg kg-1 h-1)
*
Normoxia
Hypoxia → Normoxia

Figure 3-4. Mean data and representative micrographs illustrating the effects of acclimation to hypoxia and subsequent normoxic recovery on the surface area of ionocytes (as determined using osmium-zinc iodide staining) and their distribution in goldfish (*Carassius auratus*). (A) The surface area of ionocytes was significantly decreased (indicated by asterisk) in fish exposed to hypoxia (unfilled bars) for 7 days when compared to fish kept in normoxic water (filled bars). Data are presented as means ± 1 SEM; N = 6 for all groups. (B, C) Representative light micrographs illustrate that the increase in ionocyte (arrows) surface area in fish acclimated to hypoxia for 7 days was a results of increased numbers of cells (see Table 2); scale bars: 20 μm.

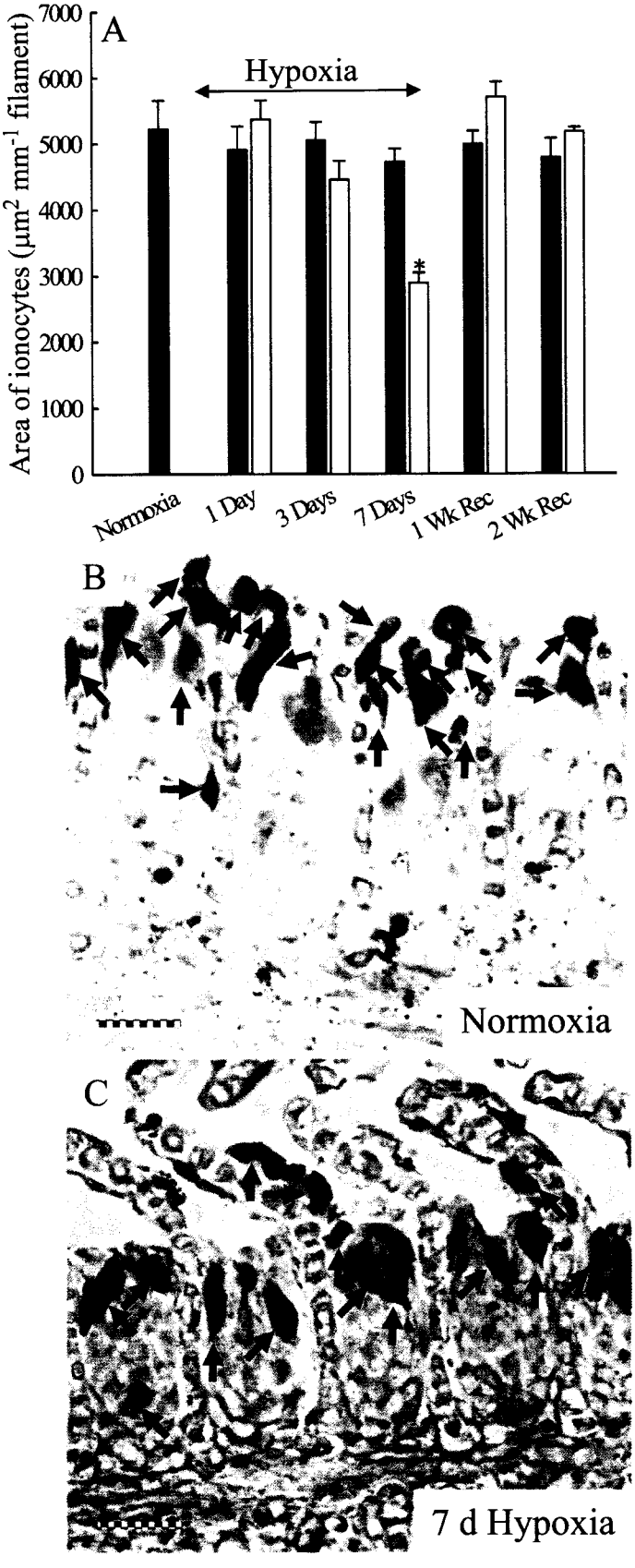
A
Hypoxia
Area of ionocytes (μm² mm⁻¹ filament)
7000
6000
5000
4000
3000
2000
1000
0
*
Normoxia
1 Day
3 Days
7 Days
1 Wk Rec
2 Wk Rec
B
Normoxia
C
7 d Hypoxia

Figure 3-5. Mean data and representative micrographs illustrating the effects of acclimation to hypoxia and subsequent normoxic recovery on the distribution of Na^+/K^+-ATPase in goldfish gill. (A) The surface area of NKA positive cells was significantly increased in fish acclimated to 3 and 7 days of hypoxia (unfilled bars). Data are presented as means ± 1 SEM. Significant differences from normoxic fish (filled bars) are indicated by asterisks ($P < 0.05$; $N = 6$ for all groups). (B, C) Representative fluorescence micrographs demonstrate that the NKA positive cells (red, arrows) remain exposed to the water regardless of the presence or absence of an interlamellar cell mass (ILCM). Cells were labeled with DAPI mounting media to show cell nuclei (blue). Scale bar: 20 μm.

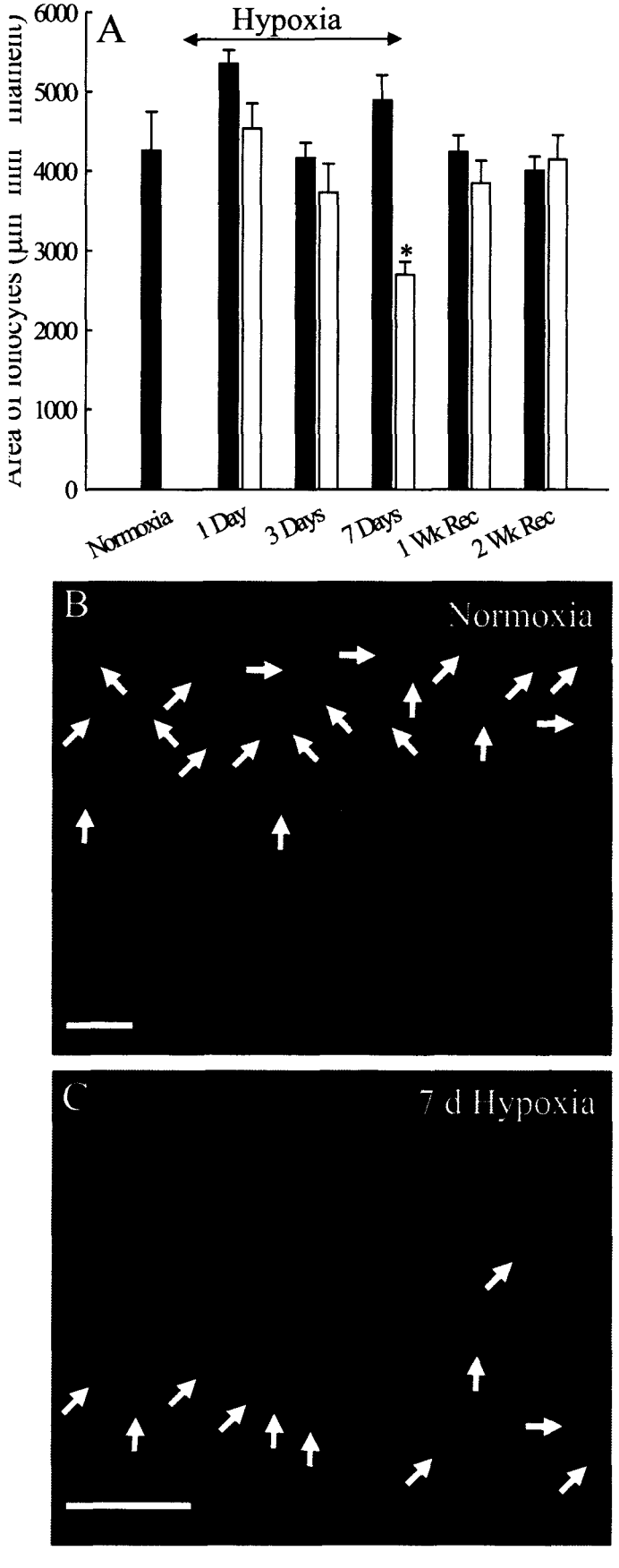
A
Hypoxia
6000
5000
4000
3000
2000
1000
0
*
Normoxia
1 Day
3 Days
7 Days
1 Wk Rec
2 Wk Rec
B
Normoxia
C
7 d Hypoxia

Figure 3-6. The effects of acclimation to hypoxia and subsequent normoxic recovery on (A) branchial Na^+/K^+-ATPase (NKA) activity and (B) relative NKA mRNA levels in goldfish (*Carassius auratus*). (A) Branchial NKA activity was increased ($P < 0.05$; indicated by asterisks) in fish exposed to 1, 3 or 7 days of hypoxia (unfilled bars; N = 6 for each group) when compared to fish acclimated to normoxia (filled bars; N = 6 for each group). (B) The expression of NKA mRNA in the fish acclimated to hypoxia (N = 6 for all groups) was significantly increased after 7 days when compared to corresponding normoxic fish (assigned a relative value of 1, N = 6 for all groups). Data are presented as means ± 1 SEM.

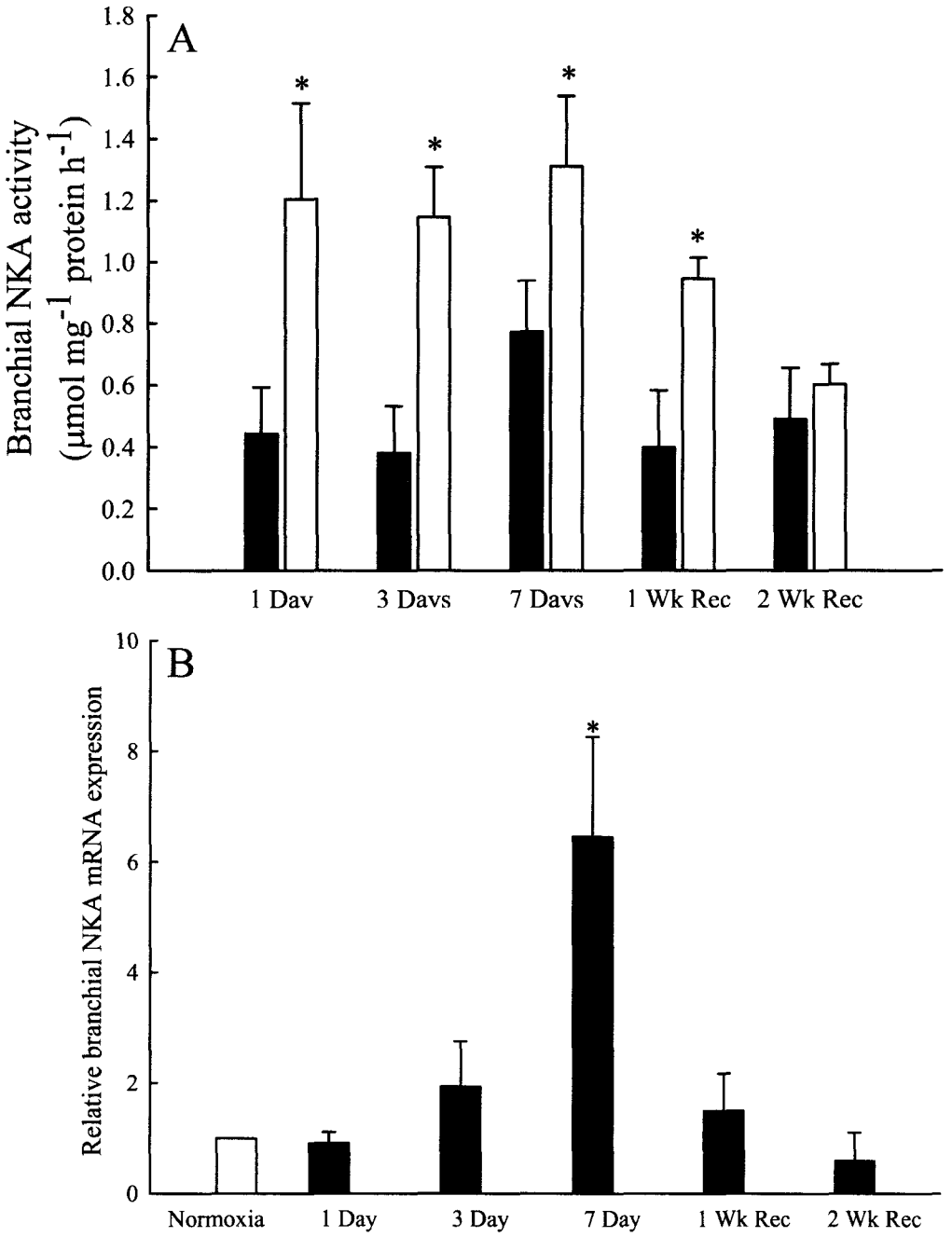
A
Branchial NKA activity
(μmol mg-1 protein h-1)
1.8
1.6
1.4
1.2
1.0
0.8
0.6
0.4
0.2
0.0
*
*
*
*
1 Dav
3 Davs
7 Davs
1 Wk Rec
2 Wk Rec
B
Relative branchial NKA mRNA expression
10
8
6
4
2
0
*
Normoxia
1 Day
3 Day
7 Day
1 Wk Rec
2 Wk Rec

Figure 3-7. The effects of hypoxia on the re-distribution of branchial ionocytes. Live fish were bathed in ^{TM}Mitotracker Red and then exposed to hypoxia for 7 days (N = 6) after which time the gills were fixed, sectioned and incubated with α5 antibody (green) to localize Na^+/K^+-ATPase positive ionocytes. Thus, after 7 days, pre-existing ionocytes would appear red (with many also staining green), while newly formed ionocytes would be single labeled and appear green only.

(A) Exposure to hypoxia resulted in a significant increase (indicated by asterisk) in the number of newly formed ionocytes (unfilled portions of bars) while the number of pre-existing ionocytes was reduced (filled portions of bars) when compared to normoxic fish. Data are presented as means ± 1 SEM.

(B, C) After 7 days, retraction of the interlamellar cell mass appeared to be accompanied by the migration of pre-existing ionocytes. Scale bar: 20 μm; cells were labeled with DAPI mounting media to show cell nuclei (blue). Newly formed ionocytes (arrows) were appearing in the ILCM. Scale bar: 20 μm; cells were labeled with DAPI mounting media to show cell nuclei (blue).

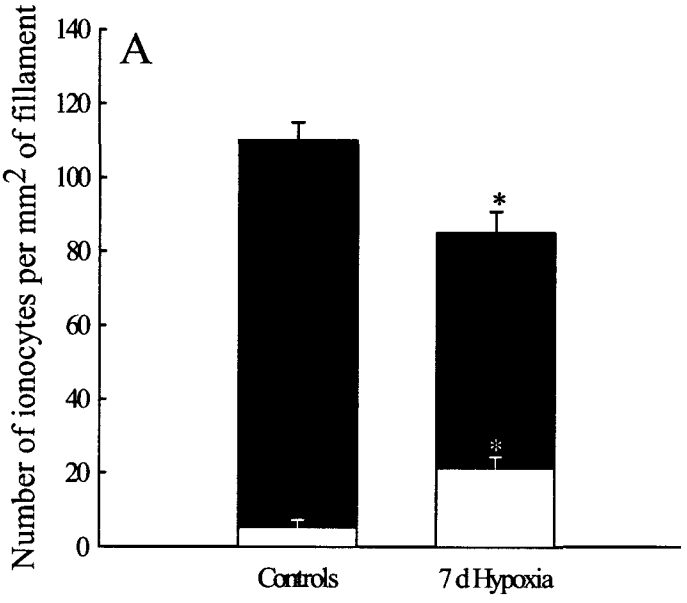
A
Number of ionocytes per mm2 of fillament
140
120
100
80
60
40
20
0
*
*
Controls
7 d Hypoxia

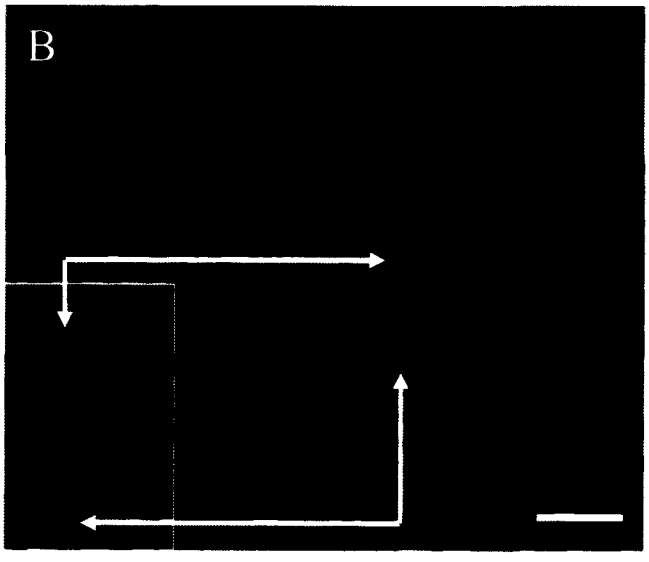
B

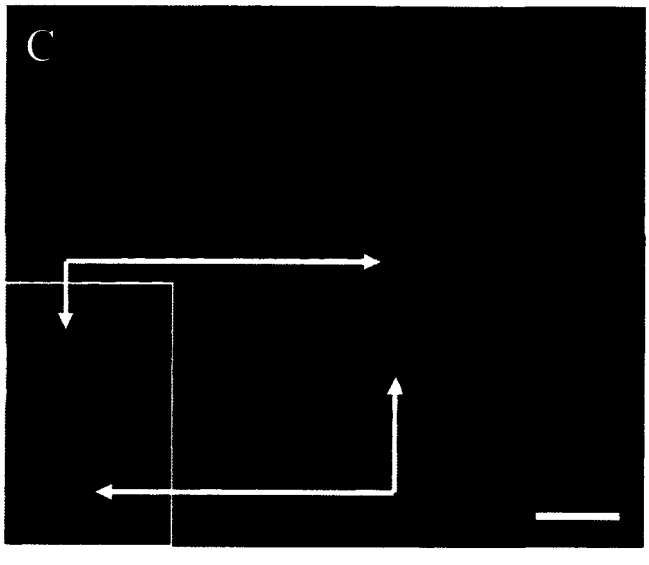
C

Table 3-1. The effects of acclimation to hypoxia and subsequent recovery on plasma Cl^- levels in goldfish (*Carassius auratus*). Data are presented as means ± 1 SEM. Significant differences from values in normoxic control fish (C) are indicated by asterisks ($P < 0.05$; $N = 6$ for all groups).

	Hypoxia (days)						Normoxic recovery (days)			
	1		3		7		7		14	
	C	H	C	H	C	H	C	H	C	H
[Cl^-] (mmol l^{-1})	91.3 ± 5.2	79.6 ± 6.9	90.5 ± 4.5	75.7 ± 5.0	93.9 ± 5.8	*67.7 ± 3.8	93.7 ± 5.3	*69.4 ± 1.8	91.7 ± 4.5	85.9 ± 4.4

Table 3-2. The effects of acclimation to hypoxia and subsequent recovery in normoxic water on the numbers and two-dimensional surface areas of individual ionocytes as identified either using osmium-zinc iodide staining or Na^+/K^+-ATPase (NKA) immunofluorescence in goldfish (*Carassius auratus*). Data are presented as means ± SEM. Significant differences from values in normoxic control fish (C) are indicated by asterisks ($P < 0.05$; $N = 6$ for all groups). The 7 day recovery samples were not analysed because of tissue deterioration.

Detection technique		**Hypoxia (days)**						**Normoxic recovery (14 days)**	
		1		**3**		**7**			
		C	H	C	H	C	H	C	H
Osmium-zinc iodide technique	Average ionocyte size (μm^2)	47.1 ± 6.1	47.7 ± 1.5	41.1 ± 1.4	36.8 ± 2.6	37.9 ± 2.7	42.0 ± 4.2	43.9 ± 2.1	47.7 ± 2.7
	Average number of ionocytes per mm of filament	105.9 ± 5.3	115.8 ± 5.8	124.7 ± 5.2	127.6 ± 8.1	128.8 ± 8.8	*71.7 ± 3.4	111.8 ± 9.4	110.5 ± 7.5
NKA immunofluorescence technique	Average ionocyte size (μm^2)	46.9 ± 4.0	36.4 ± 2.5	34.3 ± 0.9	36.8 ± 3.6	41.3 ± 2.0	34.3 ± 0.8	35.5 ± 1.1	40.0 ± 2.2
	Average number of ionocytes per mm of filament	115.6 ± 6.5	125.7 ± 3.5	121.8 ± 7.1	104.1 ± 5.6	120.4 ± 9.6	*79.9 ± 3.5	115.2 ± 4.0	114.0 ± 7.9

Discussion

The results of this study demonstrate that goldfish (*Carassius auratus*), like the related crucian carp (*Carassius carassius*) experience a gross remodeling of the gill in response to environmental hypoxia. The remodeling consists of the retraction of an interlamellar cell mass (ILCM) leading to the uncovering of previously covered lamellae and hence an increase in the functional lamellar surface area. However, unlike crucian carp, that display an ILCM over a relatively wide range of temperatures (8 – 20° C; (Sollid et al., 2003; Sollid et al., 2005), goldfish must first be acclimated to cold water (7° C in the present study) to initiate ILCM formation. Thus, unlike in crucian carp, hypoxic gill remodeling in goldfish will occur only in animals inhabiting cold water. As reported for crucian carp, the hypoxia-mediated gill remodeling was reversible upon return of goldfish to normoxia although it occurred more slowly. Goldfish required 14 days for the complete restoration of the ILCM whereas total reversal occurred in only 7 days in crucian carp acclimated to a similar temperature (8° C; Sollid et al., 2003).

Interactive effects of gill remodeling and hypoxia on branchial effluxes of Cl^- and PEG

Despite the retraction of the ILCM during hypoxia and the resultant uncovering of lamellae, there was no associated increase in the passive efflux of either Cl^- or PEG when measured under the prevailing conditions of hypoxia. Indeed, the paracellular efflux of PEG was significantly reduced in the hypoxic fish. The interpretation of these data is of course confounded by the possibility of conflicting effects of gill remodeling and hypoxia, itself. Therefore, additional experiments were performed in which hypoxic fish

were re-examined 12 h after being returned to normoxia. This brief recovery period is not long enough to allow the ILCM to regenerate (D. Mitrovic and S.F. Perry; unpublished data) but is presumed to be of sufficient duration to alleviate the acute consequences of hypoxia. The results of these experiments revealed a profound inhibitory influence of hypoxia on passive branchial fluxes because Cl^- and PEG effluxes were markedly stimulated when assayed under normoxic conditions. Thus, it is suggested that the increased surface area during hypoxic gill remodeling failed to elicit the anticipated increases in gill permeability owing to the counteracting effects of hypoxia or some secondary effect(s) associated with hypoxia. Upon removal of the hypoxia, the increase in functional surface area caused the anticipated rise in Cl^- and PEG permeability. A similar effect of short-term (6 h) hypoxia on reducing Na^+ efflux was observed in the Amazonian oscar (Wood et al., 2007). The mechanisms underlying the inhibitory effects of hypoxia on gill permeability are unknown but because Cl^- and PEG are believed to diffuse via a paracellular route, it is reasonable to assume that hypoxia is somehow "tightening" the paracellular pathways. To our knowledge, there is no prior evidence supporting such a role for hypoxia on decreasing paracellular permeability and indeed, data obtained from comparable mammalian epithelial models (e.g. the rat alveolar epithelium; Bouvry et al., 2006) demonstrate that hypoxia increases paracellular permeability by interacting with the tight junction proteins. The impact of hypoxia on tight junction proteins in the fish gill clearly is an area that warrants future research.

Another possible explanation for the reduced diffusive fluxes of PEG and Cl^- during hypoxia is that the lamellae exposed by gill remodeling do not contribute to functional surface area because they are not perfused. As discussed by Wood et al.

(2007), restricting blood flow to the gill might be advantageous for some hypoxia tolerant species exposed to such severe levels of hypoxia so as to limit ion loss and water gain in a situation where O_2 uptake is becoming futile. Whether a similar situation exists in goldfish is unclear. However, because of their high affinity hemoglobin (P_{50} = 2.6 mm Hg; Burggren, 1982) coupled with a robust hyperventilatory response (V. Tzaneva, S.F. Perry and K.M. Gilmour, unpublished data), a significant component of O_2 uptake is likely to be maintained during hypoxia. If the critical PO_2 of goldfish is similar to that of the related crucian carp at 8° C (0.5 mg l^{-1}; Sollid et al., 2003), it is likely that a significant component of aerobic metabolism was retained by the hypoxic fish in the present study.

Regardless of the mechanism(s) underlying the reduced permeability in the hypoxic goldfish, the net effect is likely to be of considerable benefit because gill surface area can be markedly increased to aid gas transfer without a major impact on osmoregulation. Notably, however, the hypoxic fish experienced significant decreases in plasma Cl^- levels suggesting negative net Cl^- balance despite the permeability adjustments of the gill. The reduction of plasma Cl^- presumably reflected the marked reduction in Cl^- uptake (see below) that was not matched by equivalent decreases in Cl^- efflux.

Interactive effects of gill remodeling and hypoxia on branchial ionocytes and influx of Cl^-

Similar to the inhibition of active Na^+ uptake observed in hypoxic Amazonian oscar (Wood et al., 2007), goldfish exposed to hypoxia exhibited a marked reduction of Cl^- uptake. While these results were unexpected given the original hypothesis of

increased Cl^- losses accompanying hypoxic gill remodeling, they were less surprising when considering that measured rates of Cl^- loss were, in fact, unaltered during hypoxia. The reduction of $J_{IN}Cl^-$ during hypoxia was likely attributable, at least in part, to a direct inhibitory effect of hypoxia because upon return to normoxia, $J_{IN}Cl^-$ was markedly stimulated. Moreover, because the rates of $J_{IN}Cl^-$ in post-hypoxic fish exceeded those in appropriate control (normoxic) fish, it would suggest that the intrinsic Cl^- transporting potential of the gill was actually increased during hypoxia but only revealed when the hypoxia was relieved. To gain insight into the possible mechanism(s) underlying the altered rates of $J_{IN}Cl^-$ during and after acclimation to hypoxia, the numbers and surface areas of ionocytes were characterized and NKA activities were assessed. Perhaps the most notable finding was that there was no obvious relationship between ionocyte abundance (and surface area) and $J_{IN}Cl^-$. In fact, when measured under normoxic conditions, the rate of $J_{IN}Cl^-$ was highest in the fish possessing fewer ionocytes. At first glance, this finding would appear to be at odds with the well known positive relationship between ionocyte abundance and rates of ionic uptake in FW fishes (Marshall et al., 1992; ; McCormick et al., 1992; Perry et al., 1992a; Perry et al., 1992b). A possible explanation for this apparent discrepancy between ionocyte abundance and J_{IN} Cl^- may be related to the location of the ionocytes. In normoxic fish at 7^{o} C, the ionocytes are found largely on the outer edge of the ILCM. Such a location of the ionocytes would presumably present a challenge for ionic uptake because the cells of the ILCM lack a blood supply (Sollid et al., 2003). Thus, the ionocytes near the center of the ILCM are likely to be uncoupled from any vascular supply. On the other hand, ionocytes at each inner edge of the ILCM may exist in close proximity to lamellar blood channels.

Ionocytes which are distant from blood channels may be inoperative or less effective at transepithelial ion uptake. It is conceivable therefore, that increased numbers of ionocytes are required in the normoxic fish to sustain required rates of $J_{IN}Cl^-$. In the hypoxic fish, the ionocytes tend to be in closer proximity to lamellae (e.g. see Fig. 7) and may be more effective in the translocation of Cl^- thus requiring fewer numbers of participating cells.

Two different procedures were used to quantify the numbers and surface areas of ionocytes; staining using Champ-Maillet's fixative (Garcia-Romeu and Masoni, 1970) and NKA immunofluorescence. Each technique is believed to specifically stain cells with enriched basolateral membranes because of their high phospholipid content (Champ-Maillet's fixative) and abundance of NKA (immunofluorescence). It is conceivable, however, that some types of ionocytes cannot be identified using either of these techniques. For example, the cuboidal cells of *Fundulus heteroclitus* (Laurent et al., 2006) and the PNA^- MRCs of rainbow trout (*Oncorhynchus mykiss*) (Galvez et al., 2002; Goss et al., 2001), both believed to be examples of ionocytes, lacking a distinct tubulo-vesicular system. Such ionocytes can be identified, at least in part, on the basis of their abundant mitochondria. Despite the fewer numbers of ionocytes in the hypoxic fish, branchial NKA activity was significantly elevated, presumably a reflection of the increased levels of NKA mRNA. The simplest explanation for these data is that the amount of NKA per ionocyte was increasing to counteract the inhibitory effects of hypoxia on NKA activity (Bogdanova et al., 2005). Because NKA activity was determined under optimal normoxic conditions, the inhibitory effects of hypoxia would not have been observed in the *in vitro* assays. It is possible that the increasing levels of

NKA in the hypoxic fish returned to normoxia were contributing to the increased rates of $J_{IN}Cl^-$ measured at this time. Hypoxia might also have a regulatory role on the effect on the phosphorylation of the NKA thus being able to rapidly influence its activity (Tipsmark and Madsen, 2001).

The finding of increased NKA levels in hypoxic goldfish was in striking contrast to results reported in a recent study on the Amazonian oscar (*Astronotus ocellatus*) in which NKA activity was found to decrease significantly during hypoxia (Wood et al., 2007). A potential explanation for the discrepancy between the two studies is that the goldfish (this study) were exposed to hypoxia for 1 – 7 days whereas the oscars were exposed for only 6 h (Wood et al., 2007). While likely inhibiting NKA activity, it is also possible that hypoxia was specifically influencing the *in vivo* functioning of one or more ion transport proteins involved in Cl^- uptake. Currently, the molecular mechanisms of Cl^- uptake across the fish gill are unknown although several anion transport proteins have been suggested to be involved including SLC26A4 (pendrin; Piermarini et al., 2002) and SLC4A1 (AE1; Wilson et al., 2000).

The mechanisms of ionocyte redistribution during hypoxic remodeling of the gill

In the present study, we adapted the "time-differential double fluorescent staining" technique of Katoh and Kaneko (2003) to study the kinetics of ionocyte redistribution associated with remodeling of the gill in goldfish exposed to hypoxia. The intent was to determine the relative importance of cell migration and cell differentiation to the redistribution of ionocytes as the ILCM was retracted during hypoxia. The method of Katoh and Kaneko (2003) used two fluorescent mitochondrial indicator dyes

(^{TM}Mitotracker red and ^{TM}Mitotracker green) to identify pre-existing and newly formed ionocytes. While we were able to achieve reliable and long-lasting (2 weeks) staining by bathing fish *in vivo* with ^{TM}Mitotracker red, we were unsuccessful when using a second application of ^{TM}Mitotracker green 7 days later. Thus, it was necessary to modify the published procedure of Katoh and Kaneko (2003). This was accomplished by applying an antibody (α5 monoclonal antibody) to localize NKA on tissue sections derived from fish previously treated with ^{TM}Mitotracker red (two weeks earlier). The interpretation of these data relies on the basic assumption that ^{TM}Mitotracker and the NKA antibody are in fact labeling the same cell type. We believe that this is a reasonable assumption especially given the similar changes in ionocyte numbers and surface areas during hypoxia exposure as determined using the two different techniques (Table 3-2). While all cells positive for NKA are likely to be ionocytes, there may be a sub-set of ionocytes that are not enriched with NKA as observed for the H^+-ATPase enriched ionocytes of zebrafish larvae (Hwang and Lee, 2007). Even if such cells were present in goldfish, the conclusions regarding cell migration and differentiation would still hold given the probability that all NKA positive cells are ion transporting cells (ionocytes).

By using the "time-dependent double fluorescent staining technique" it was determined that ionocytes present on the outer edge of the ILCM in normoxic fish simply migrated with the diminishing ILCM during hypoxia so as to remain in contact with the water. Limitations of the technique (it is not possible to view "before" and "after" images from the same fish) did not allow us to calculate the exact percentage of ionocytes migrating over the 7-day period of hypoxia. However, a comparison of ionocyte numbers on the ILCM of normoxic and hypoxic fish suggest that the vast majority of

cells migrated and that only a small fraction were removed or newly formed. This raises questions as to the physical nature of the ILCM remodeling and suggests that the ILCM retracts in a regulated manner to specifically maintain the population of ion-transporting cells. While the newly differentiated ionocytes observed within the ILCM presumably were derived from resident stem cells, the exact origin of these progenitor cells is unknown. Other studies, however, have demonstrated that ionocytes appearing on the lamellae are derived from stem cells within the filament (Laurent et al., 1995) and thus the appearance of newly differentiated ionocytes in the ILCM of goldfish may reflect a similar process.

Perspectives

Gross remodeling of the gill in crucian carp and goldfish is used as a strategy to match functional lamellar surface area with gas transfer or metabolic requirements so as to minimize the obligatory diffusive movements of salts and water (the osmorespiratory compromise). In the natural environment, such a strategy may be energetically beneficial if the costs associated with replenishing the ILCM do not exceed the additional energy expenditure that otherwise would be incurred by replacing the lost salt or voiding the gained water. Traditionally, the energetic cost of osmotic regulation in freshwater fish is estimated to be <5% of overall metabolic rate (Morgan and Iwama, 1999). However, the results of the present study and those of Wood et al. (2007) suggest that the additional metabolic costs of ionic regulation incurred by increasing functional lamellar surface area may not necessarily be as high as historically predicted by the osmorespiratory compromise. For example, in goldfish acclimated to 7° C, the retraction of the ILCM

during hypoxia does not lead to an increase in the passive efflux of Cl^- or the paracellular marker PEG despite a marked increase in functional lamellar surface area. This is likely an adaptive response that has evolved in hypoxia tolerant species such as goldfish and oscar (Vanwaversveld et al., 1989) to reduce osmoregulatory costs without simultaneously impeding branchial oxygen uptake. Future research should be directed at elucidating the mechanisms underlying the apparent reduction in branchial permeability during hypoxic gill remodeling.

CHAPTER 4

GENERAL DISCUSSION

This thesis aimed to investigate the physiological consequences of gill remodeling in the goldfish (*Carassius auratus*) caused either by temperature change or by exposure to hypoxia. The results confirmed previous findings of Sollid et al. (2003, 2005, 2006) which demonstrated that gill surface area (SA) in crucian carp is plastic owing to the expansion or retraction of an interlamellar cell mass (ILCM). The present study, while providing the first evidence for morphological remodeling of the goldfish gill during exposure to hypoxia also provided insight into the functioning of the gill under such periods of remodeling. A major aim of this thesis was to show how modification of the gill surface area affects Cl^- balance. The results demonstrated a decrease in the number of ion-transporting ionocytes under conditions of increased gill surface area, an unexpected finding. However, an explanation for the decreased SA of ionocytes may be related to their position relative to the ILCM. In a situation of increased temperature ionocytes were more exposed to the surrounding water environment and were also closer to the vascularised tissue making them more efficient, thus their reduced SA. The mismatch between the SA of the ionocytes (deduced by both the surface area of MRC and NKA positive cells) and NKA activity might suggest that more than one process is responsible for Cl^- balance within a goldfish (Chapter 2 and Chapter 3). Also, in hypoxic fish experiencing increased gill surface area, the passive loss of Cl^- appears to be restricted by hypoxia, itself, where the presence of the hypoxic conditions minimizes the movement of Cl^- ions in either direction and these effects are diminished with the return of normoxia.

Effects of temperature change or hypoxia on gill morphology

Chapter 2 focused on temperature induced morphological changes on the functioning of the gill. The two temperatures (7 and 25° C) were chosen to reflect the extremes of natural conditions and to yield two distinct phenotypes exhibiting a large variation in branchial lamellar functional surface area, where warm temperature will result in large functional surface area (SA) while gills from cold water will have a small functional SA due to the large presence of ILCM. The effects of hypoxia exposure on the morphology of the gill and the resulting functional alterations were evaluated in Chapter 3. The functional surface area of exposed lamellae appeared to be directly proportional to the duration of hypoxia because of a gradual decrease in the area of the ILCM. The initial component of this study examined morphological changes, due to either temperature change or exposure to hypoxia, of the cells (ionocytes) thought to be responsible for Cl^- uptake in freshwater fish. Previous research (Sollid et al., 2005) has already shown that the morphological changes due to hypoxia in crucian carp are reversible and our results indicate that the same was true for goldfish as the ILCM reformed once the fish were returned to normoxic water. With the movement of the ILCM due to temperature decrease or return to normoxia, there also seemed to be a movement of the majority of the pre existing ionocytes because they are predominantly found at the edge of the ILCM exposed to the water regardless of the area occupied by the ILCM thus are always somewhat capable of operating. As a consequence of migration of the pre-existing cells and to a lesser extent some differentiation of stem cells, the branchial ionocytes remained largely exposed to the water regardless of the presence or absence of an ILCM in either situation. The "time-differential double

fluorescent staining" protocol provided some insight into the replenishment of the ionocytes. As was observed in fish acclimated to differing temperatures (Chapter 2) or hypoxia exposure and recovery (Chapter 3), the ionocytes remained mostly on the outer edge of the ILCM because they simply migrated with the ILCM as it retracted or expanded. In addition, new cells were occasionally formed which tended to be found underneath the ILCM.

The decrease that was observed in the SA of the ionocytes accompanied by larger exposure of these cells to the water (they were outside of the ILCM more often) was not consistent with the assumption that with increased lamellar SA, an increase in passive ion loss would be countered by higher rates of ion absorption. Furthermore, the decrease in the SA of the ionocytes (despite the associated rise in NKA activity) due to the increased exposure of these cells to the water as the functional SA of the gill increased suggests that these cells are performing at a higher efficiency in order to compensate for elevated rates of ion loss so as to maintain a stable internal environment. However, despite these lower numbers of ionocytes and increased NKA activity, there was no accompanying change in the Cl^- uptake at a higher water temperature. These results suggest that ionocytes may be involved in Na^+ or Ca^{2+} rather than Cl^- uptake or that there are multiple processes responsible for Cl^- balance.

Effects of temperature or hypoxia on Cl^- fluxes

The second component of this study focused more specifically on the impact of changing surface area of the gill on Cl^- balance. Even though there was a marked increase in the paracellular permeability of the gill (as indicated in the PEG

experiment) due to increase in temperature which resulted in the increased functional SA there was no increase in Cl^- efflux. The large difference in lamellar functional surface area in the fish acclimated to 7 or 25° C resulted in a markedly increased branchial efflux of the paracellular flux marker PEG (Wood et al., 1998) in the warm water acclimated fish. There seems to exist a linear relationship between the increase in functional SA and equivalent increase in PEG efflux, indicating that the alterations of the gill due to acclimation of temperature is only reflected in the increased functional surface area. On the other hand, the much smaller increase of the paracellular efflux of Cl^- at higher temperature in response to the same increase of functional surface area as for PEG provides evidence for a specific regulation of Cl^- permeability as surface area increases so as to minimize the paracellular loss of Cl^-. However, because Cl^- efflux in warm water acclimated fish exceeds influx and the fish are faced with a negative Cl^- balance, a new steady state levels of plasma Cl^- can only be achieved via supplementary dietary uptake of Cl^-.

The second half of Chapter 3 examined the effects of hypoxia on Cl^- balance. When fish acclimated to 7 days hypoxia were compared to normoxic fish, there was no significant difference in the rates of Cl^- loss (passive) or uptake (active) even though the functional SA of the gill appeared to be extremely different between the two groups. The increase of the functional SA, observed with the increase in hypoxia duration, did not mimic the similar alterations seen with the increase in temperature. Thus, the increase in functional surface area coupled with hypoxia appears to have a regulated effect on both passive Cl^- loss as well as active Cl^- gain because $J_{OUT}Cl^-$ was unchanged and $J_{IN}Cl^-$ was actually reduced when compared to normoxic counterparts. The lack of increase of

passive ion loss was further supported by the decrease in paracellular permeability, suggesting that the overall gill became tighter thus reducing passive paracellular movements. The opposite effect of the increase of lamellar SA on PEG fluxes was observed in temperature situation.

When the specific effects of hypoxia were taken out of the equation and the consequences of increased functional surface area on Cl^- and PEG fluxes were re-evaluated under normoxic conditions, the expected results that match the temperature situation were observed. An increase in passive Cl^- loss and active Cl^- uptake was observed in hypoxic fish that were allowed to recover for 12 h in normoxic water. Without the confounding influence of hypoxia the increased functional SA was associated with the expected large increases in Cl^- and PEG effluxes. There have been reports of similar findings in the recent literature where it was suggested that hypoxia induces flux arrest (similar to channel arrest in neurons) in gills of hypoxic fish (Wood et al., 2007; Scott et al., 2008). It has been suggested that the hypoxia tolerant Amazonian oscar (*Astonotus ocellatus*) is able to survive hypoxic conditions owing to pronounced suppression of oxygen needs rather than by attempting to maximize O_2 uptake (Scott et al., 2008). Judging from the Cl^- flux data, it can be concluded that goldfish also experience "flux arrest". The strategy used by goldfish exposed to hypoxia is to limit Cl^- loss to reduce the need for costly Cl^- uptake.

Collectively lowering the Cl^- diffusion gradient and selective "tightening" of the paracellular pathways through the tight junctions to Cl^-, provide an effective strategy to reduce the costs of absorbing Cl^- in fish with increased functional surface area due to the exposure of hypoxia or temperature alterations.

Future directions

Further research can take a number of different paths in order to answer many of the questions posed by this thesis. Future work needs to characterize the metabolic costs of ILCM production and maintenance. The characterization of the ionocytes of the goldfish gills should be a priority, which would provide direct evidence for ionocyte subtype presence and function as they may relate to ion regulation. A more focused future direction might look at the effects of hypoxia on other ion fluxes such as Na^+ and Ca^{2+}, and the effects of their imbalance on the morphology of the gill. Also, further studies are required to explain the apparent discrepancy between rates of Cl^- uptake and blood supply in the goldfish possessing an ILCM. Another direction may lead to answer the question of the exact function of the ionocytes, as well as indentifying the cells and/or ion channels that are responsible for Cl^- uptake if it is shown that those are not ionocytes. A different direction further research can take is to closely examine the effects of tight junctions between the cell of the gill as well as the cells of the ILCM and what controls their behaviour and abundance in response to the functional SA changes. The ILCM does not appear to be innervated yet it is dynamic in nature as well as the ionocytes that are embedded within it, so a closer examination of how these cells receive their molecular messages and where they come from is in order.

References

Alexandre, M. D., Lu, Q., and Chen, Y. H. (2005). Overexpression of claudin-7 decreases the paracellular Cl- conductance and increases the paracellular Na^+ conductance in LLC-PK1 cells. J Cell Sci **118**, 2683-2693.

Anderson, J. M., Van Itallie, C. M., and Fanning, A. S. (2004). Setting up a selective barrier at the apical junction complex. Curr. Opin. Cell Biol **16**, 140-145.

Bagherie-Lachidan, M., Wright, S. I., and Kelly, S. P. (2008). Claudin-3 tight junction proteins in Tetraodon nigroviridis: cloning, tissue-specific expression, and a role in hydromineral balance. Am J Physiol **294**, R1638-R1647.

Bickler, P. E., Donohoe, P. H., and Buck, L. T. (2000). Hypoxia-induced silencing of NMDA receptors in turtle neurons. J Neurosci **20(10)**, 3522-3528.

Bogdanova, A., Grenacher, B., Nikinmaa, M., and Gassmann M. (2005). Hypoxic responses of Na+/K+ ATPase in trout hepatocytes. J Exp Biol **208**, 1793-1801.

Booth, J. H. (1979). Circulation in trout gills: the relationship between branchial perfusion and the width of the lamellar blood space. Can J Zool **57**, 2183-2185.

Bouvry D., Planès, C., Malbert-Colas, L., Escabasse, V., and Clerici, C. (2006). Hypoxia-induced cytoskeleton disruption in alveolar epithelial cells. Am J Respir Cell Mol Biol **35(5)**, 519-527.

Brauner, C. J., Matey, V., Wilson, J. M., Bernier, N. J., and Val, A. L. (2004). Transition in organ function during the evolution of air-breathing; insights from Arapaima gigas, an obligate air-breathing teleost from the Amazon. J Exp Biol **207**, 1433-1438.

Burggren, W. W. (1982). Pulmonary Blood Plasma Filtration in Reptiles: A "Wet" Vertebrate Lung? Science **215(4528)**, 77-78.

Burggren, WW. (1982). "Air gulping" improves blood oxygen transport during aquatic hypoxia in the goldfish Carassius auratus. Physiol Zool **55**, 327-334.

Burleson, M. L. (1995). Oxygen availability: Sensory systems. In Biochemistry and molecular biology of fishes (eds. P. W. Hochachka and T. P. Mommsen), pp. 1-18. Amsterdam: Elsevier.

Burleson, M. L., Mercer, S. E., and Wilk-Blaszczak, M. A. (2006). Isolation and characterization of putative O2 chemoreceptor cells from the gills of channel catfish (Ictalurus punctatus). Brain Res **1092**, 100-107.

Burleson, M. L., Smatresk, N. J., and Milsom, W. K. (1992). Afferent inputs associated with cardioventilatory control in fish. In The Cardiovascular System (eds. W. S. Hoar, D. J. Randall, and A. P. Farrell), pp. 389-423. San Diego: Academic Press.

Chasiotis, H. and Kelly, S. P. (2008). Occludin immunolocalization and protein expression in goldfish. J Exp Biol 211, 1524-1534.

Chou, M. Y., Hsiao, C. D., Chen, S. C., Chen, I. W., Liu, S. T., and Hwang, P. P. (2008). Effects of hypothermia on gene expression in zebrafish gills: upregulation in differentiation and function of ionocytes as compensatory responses. J. Exp. Biol. 211, 3077-3084.

Chretien, M. and Pisam, M. (1986). Cell renewal and differentiation in the gill epithelium of fresh- or salt-water-adapted euryhaline fosh as revealed by [3H]- thymidine radioautography. Biol Cell 56, 137-150.

Claiborne, J. B. (1998). Acid-base regulation. In: The Physiology of Fishes vol. 2, Ed. D.H. Evans, CRC Press, Boca Ratan., 171-198.

Claiborne, J. B., Choe, K. P., Morrison-Shetlar, A. I., Weakley, J. C., Havird, J., Freiji, A., Evans, D. H., and Edwards, S. L. (2008). Molecular detection and immunological localization of gill Na+/H+ exchanger in the dogfish (Squalus acanthias). Am J Physiol 294, R1092-R1102.

De Fraga, L. S., Da Silva, R. S., Achaval, M., and Zancan D. M. (2004). Carbohydrate metabolism in the central nervous system of the megalobulimus oblongus snail during anoxia exposure and post-anoxia recovery. J Exp Zoolog A Comp Exp Biol 301(12), 968-978.

De Renzis, G. and Maetz, J. (1973). Studies on the mechanism of chloride absorption by the goldfish gill: relation with acid-base regulation. J Exp Biol 59, 339-358.

Evans, D. H., Piermarini, P. M., and Choe, K. P. (2005). The multifunctional fish gill: dominant site of gas exchange, osmoregulation, acid-base regulation, and excretion of nitrogenous waste. Physiol Rev 85, 97-177.

Evans, D. H., Piermarini, P. M., and Potts, W. T. W. (1999). Ionic transport in the fish gill epithelium. J Exp Zool **283**, 641-652.

Farrell, A. P., Sobin, S. S., Randall, D. J., and Crosby, S. (1980). Intralamellar blood flow patterns in fish gills. Am J Physiol **239**, R428-R436.

Galvez F, Reid SD, Hawkings G and Goss GG. (2002). Isolation and characterization of mitochondria-rich cell types from the gill of freshwater rainbow trout. *Am J Physiol* 282: R658-R668.

Garcia-Romeu, F. and Masoni, A. (1970). Sur la mise en evidence des cellules a chlorure de la branchie des poissons. Arch Anat Microsc **59**, 289-294.

Gilmour, K. M. (1997). Gas exchange. In The Physiology of Fishes (ed. D. H. Evans), pp. 101-127. Boca Raton: CRC Press.

Gilmour, K. M. and Perry, S. F. (2007). Branchial Chemoreceptor Regulation of Cardiorespiratory Function. In Sensory Systems Neuroscience (eds. T. J. Hara and B. Zielinski), pp. 97-151. Academic Press.

Gonzalez-Mariscal, L., Betanzos, A., Nava, P., and Jaramillo, B. E. (2003). Tight junction proteins. Prog Biophys Mol Biol **81**, 1-44.

Gonzalez, R. J., and McDonald, D. G. (1992). The relationship between oxygen consumption and ion loss in a freshwater fish. J Exp Biol **163**, 317-332.

Goss, G. G., Adamia, S., and Galvez, F. (2001). Peanut lectin binds to a subpopulation of mitochondria-rich cells in the rainbow trout gill epithelium. Am J Physiol **281**, R1718-R1725.

Goss, G. G., Perry, S. F., Wood, C. M., and Laurent, P. (1992). Mechansisms of ion and acid-base regulation at the gills of freshwater fish. J Exp Zool **263**, 143-159.

Hyvärinen, L., Lindstedt, E., Laurinen, P., and Nyman, G. (1985). Visual illusion mimicking dyslexia. A case history. Acta Ophthalmol (Copenh) **63(5),** 588-590.

Hiroi, J., Yasumasu, S., McCormick, S. D., Hwang, P.-P., and Kaneko, T. (2008). Evidence for an apical Na-Cl cotransporter involved in ion uptake in a teleost fish. J Exp Biol **211**, 2584-2599.

Horng, J. L., Lin, L. Y., Huang, C. J., Katoh, F., Kaneko, T., and Hwang, P. P. (2007). Knockdown of V-ATPase subunit A (atp6v1a) impairs acid secretion and ion balance in zebrafish (Danio rerio). Am J Physiol **292**, R2068-R2076.

Hwang, P. P. and Lee, T. H. (2007). New insights into fish ion regulation and mitochondrion-rich cells. Comp Biochem. Physiol A **148**, 479-497.

Jonz, M. G., Fearon, I. M., and Nurse, C. A. (2004). Neuroepithelial oxygen chemoreceptors of the zebrafish gill. J Physiol **560**, 737-752.

Katoh, F. and Kaneko, T. (2003). Short-term transformation and long-term replacement of branchial chloride cells in killifish transferred from seawater to freshwater, revealed by morphofunctional observations and a newly established 'time-differential double fluorescent staining' technique. J Exp Biol **206**, 4113-4123.

Laurent, P. (1984). Gill internal morphology. In Fish Physiology Vol XA (eds. W. S. Hoar and D. J. Randall), pp. 73-183. New York: Academic Press.

Laurent, P., Chevalier, C., and Wood, C. M. (2006). Appearance of cuboidal cells in relation to salinity in gills of Fundulus heteroclitus, a species exhibiting branchial Na^+ but not Cl^- uptake in freshwater. Cell Tissue Res **325**, 481-492.

Laurent, P. and Dunel, S. (1980). Morphology of gill epithelia in fish. Am J Physiol **238**, R147-R159.

Laurent, P. L., Dunel-Erb, S., Chevalier, C., and Lignon, J. (1995). Gill epithelial cell kinetics in a freshwater teleost, Oncorhynchus mykiss, during adaptation to ion-poor water and hormonal treatments. Fish Physiol Biochem **13**, 353-370.

Lin, L. Y., Horng, J. L., Kunkel, J. G., and Hwang, P. P. (2006). Proton pump-rich cell secretes acid in skin of zebrafish larvae. Am J Physiol **290**, C371-C378.

Lundgreen, K., Kiilerich, P., Tipsmark, C. K., Madsen, S. S., and Jensen, F. B. (2008). Physiological response in the European flounder (Platichthys flesus) to variable salinity and oxygen conditions. J Comp Physiol [B] **178**, 909-915.

Maetz, J. and Garcia Romeu, F. (1964). The Mechanism of Sodium and Chloride Uptake by the Gills of a Fresh-Water Fish, Carassius auratus: II. Evidence for NH_4^+ / Na^+ and HCO_3^- / Cl^- exchanges. J Gen Physiol **47**, 1209-1227.

Marshall, W. S. and Grosell, M. (2006). Ion transport, osmoregulation and acid-base balance. In The Physiology of Fishes (eds. D. H. Evans and J. B. Claiborne), pp. 177-230. Boca Raton: CRC Press.

Marshall, W. S., Bryson, S. E., and Wood, C. M. (1992). Calcium transport by isolated skin of rainbow trout. *J Exp Biol* **166**, 297-316.

McCormick, S.D., Hasegawa, S., and Hirano, T. (1992). Calcium uptake in the skin of a freshwater teleost. Proc Natl Acad Sci U S A **89**, 3635-3638.

McCormick, S. D. (1993). Methods for non-lethal gill biopsy and measurements of Na^+,K^+-ATPase activity. *Can J Fish Aquat Sci* **50**, 656-658.

McCormick, S. D. (1995). Hormonal control of gill Na^+,K^+-ATPase and chloride cell function. In *Fish Physiology Vol 14; Cellular and Molecular Approaches to Fish Ionic Regulation* (eds. C.M. Wood and T.J. Shuttleworth) pp 285-315, Academic Press, New York.

Metz, J. R., van den Burg, E. H., Bonga, S. E., and Flik, G. (2003). Regulation of branchial Na+/K+-ATPase in common carp Cyprinus carpio L. acclimated to different temperatures. J Exp Biol 206, 2273-2280.

Morgan JD and Iwama GK. (1999). Energy cost of NaCl transport in isolated gills of cutthroat trout. Am J Physiol 99: 631-639.

Murphy, P. G. and Houston, A. H. (1974). Environmental temperature and the body fluid system of the fresh-water teleost V. Plasma electrolyte levels and branchial microsomal (Na+-K+) ATPase activity in thermally acclimated goldfish (Carassius auratus). Comp Biochem Physiol **B 47**, 563-570.

Nikinmaa, M. (2006). Gas Transport. In The Physiology of Fishes (eds. D. H. Evans and J. B. Claiborne), pp. 153-174. Boca Raton: CRC Press.

Nilsson, G. E. (2007). Gill remodeling in fish-a new fashion or an ancient secret? J Exp Biol **210**, 2403-2409.

Nilsson, G. E., Renshaw, G. M. (2004). Hypoxic survival strategies in two fishes: extreme anoxia tolerance in the North European crucian carp and natural hypoxic preconditioning in a coral-reef shark. J Exp Biol **207(Pt 18)**, 3131-3139.

Nilsson, G. E. (1990). Long-term anoxia in crucian carp: changes in the levels of amino acid and monoamine neurotransmitters in the brain, catecholamines in chromaffin tissue, and liver glycogen. J Exp Biol **150 (1)**, 295-320.

Olson, K. R. (1998). Hormone metabolism by the fish gill. Comp Biochem Physiol **119A**, 55-65.

Olson, K. R. (2002). Gill circulation: Regulation of perfusion distribution and metabolism of regulatory molecules. J Exp Zool **293**, 320-335.

Ong, K. J., Stevens, E. D., and Wright, P. A. (2007). Gill morphology of the mangrove killifish (Kryptolebias marmoratus) is plastic and changes in response to terrestrial air exposure. J Exp Biol **210**, 1109-1115.

Parks, S. K., Tresguerres, M., and Goss, G. G. (2007). Interactions between Na+ channels and Na^+-HCO_3^- cotransporters in the freshwater fish gill MR cell: a model for transepithelial Na+ uptake. Am J Physiol **292**, C935-C944.

Perry, S. F. (1997). The chloride cell: Structure and function in the gill of freshwater fishes. Annu Rev Physiol **59**, 325-347.

Perry, S. F., Furimsky, M., Bayaa, M., Georgalis, T., Nickerson, J. G., and Moon, T. W. (2003a). Integrated involvement of Na+/HCO3- cotransporters and V-type H^+-ATPases in branchial and renal acid-base regulation in freshwater fishes. Biochem Biophys Acta **1618**, 175-184.

Perry, S. F., Shahsavarani, A., Georgalis, T., Bayaa, M., Furimsky, M., and Thomas, S. L. Y. (2003b). Channels, pumps and exchangers in the gill and kidney of freshwater fishes: Their role in ionic and acid-base regulation. J Exp Zool **300**, 53-62.

Perry, S. F. and Gilmour, K. M. (2002). Sensing and transfer of respiratory gases at the fish gill. J Exp Zool **293**, 249-263.

Perry, S. F. and Gilmour, K. M. (2006). Acid-base balance and CO_2 excretion in fish: Unanswered questions and emerging models. Respir Physiol Neurobiol **154**, 199-215.

Perry, S. F., Goss, G. G., and Fenwick, J. C. (1992a). Interrelationships between gill chloride cell morphology and calcium uptake in freshwater teleosts. *Fish Physiol Biochem* **10**, 327-337.

Perry, S. F., Goss, G. G., and Laurent, P. (1992b). The interrelationships between gill chloride cell morphology and ionic uptake in four freshwater teleosts. *Can J Zool* **70**, 1737-1742.

Perry, S. F. and McDonald, D. G. (1993). Gas Exchange. In The Physiology of Fishes (ed. D. H. Evans), pp. 251-278. Boca Raton, Florida: CRC Press.

Pfaffl, M. W. (2001). A new mathematical model for relative quantification in real-time RT-PCR. Nucl Acids Res **29**, 2002-2007.

Piermarini, P. M., Verlander, J. W., Royaux, I. E., and Evans, D. H. (2002). Pendrin immunoreactivity in the gill epithelium of a euryhaline elasmobranch. Am J Physiol **283**, R983-R992.

Preest, M. R., Gonzalez, R. J., and Wilson, R. W. (2005). A pharmacological examination of Na^+ and Cl^- transport in two species of freshwater fish. Physiol Biochem Zool **78**, 259-272.

Randall, D. J. and Daxboeck, C. (1984). Oxygen and carbon dioxide transfer across fish gills. In Fish Physiology (eds. W. S. Hoar and D. J. Randall), pp. 263-314. New York: Academic Press.

Randall, D. J., Baumgarten, D., and Malyusz, M. (1972). The relationship between gas and ion transfer across the gills of fishes. Comp Biochem Physiol A **41**, 629-637.

Reid, S. D., Hawkings, G. S., Galvez, F., and Goss, G. G. (2003). Localization and characterization of phenamil-sensitive Na^+ influx in isolated rainbow trout gill epithelial cells. J Exp Biol **206**, 551-559.

Sloman, K. A., Desforges, P. R., and Gilmour, K. M. (2001). Evidence for a mineralocorticoid-like receptor linked to branchial chloride cell proliferation in freshwater rainbow trout. *J Exp Biol* **204**, 3953-3961.

Stensløkken, K., Milton, S. L., Lutz, P. L., Sundin, L., Renshaw, G. M. C., Stecyk, J. A.W., and Nilsson, G. E. (2008). Effect of anoxia on the electroretinogram of three anoxia-tolerant vertebrates. Comp Biochem Physiol A Mol Integr Physiol **150(4)**, 395-403.

Scott, G. R., Wood, C. M., Sloman, K. A., Iftikar, F. I., De Boeck, G., Almeida-Val, V. M., and Val, A. L. (2008). Respiratory responses to progressive hypoxia in the Amazonian oscar, Astronotus ocellatus. Respir Physiol Neurobiol **162(2)**, 109-116.

Sollid, J., De Angelis, P., Gundersen, K., and Nilsson, G. E. (2003). Hypoxia induces adaptive and reversible gross morphological changes in crucian carp gills. J Exp Biol **206**, 3667-3673.

Sollid, J. and Nilsson, G. E. (2006). Plasticity of respiratory structures-adaptive remodeling of fish gills induced by ambient oxygen and temperature. Respir Physiol Neurobiol **154**, 241-251.

Sollid, J., Weber, R. E., and Nilsson, G. E. (2005). Temperature alters the respiratory surface area of crucian carp Carassius carassius and goldfish Carassius auratus. J Exp Biol **208**, 1109-1116.

Tipsmark, C. K., Baltzegar, D. A., Ozden, O., Grubb, B. J., and Borski, R. J. (2008a). Salinity regulates claudin mRNA and protein expression in the teleost gill. Am J Physiol **294**, R1004-R1014.

Tipsmark, C. K., Kiilerich, P., Nilsen, T. O., Ebbesson, L. O., Stefansson, S. O., and Madsen, S. S. (2008b). Branchial expression patterns of claudin isoforms in Atlantic salmon during seawater acclimation and smoltification. Am J Physiol **294**, R1563-R1574.

Tipsmark, C. K., Luckenbach, J. A., Madsen, S. S., Kiilerich, P., and Borski, R. J. (2008c). Osmoregulation and expression of ion transport proteins and putative claudins in the gill of southern flounder (Paralichthys lethostigma). Comp Biochem Physiol **150**, 265-273.

Tipsmark, C. K. and Madsen, S. S. (2001). Rapid modulation of Na+/K+-ATPase activity in osmoregulatory tissues of a salmonid fish. J Exp Biol **204 (Pt 4)**:701-709.

Tresguerres, M., Katoh, F., Orr, E., Parks, S. K., and Goss, G. G. (2006). Chloride uptake and base secretion in freshwater fish: a transepithelial ion-transport metabolon? Physiol Biochem Zool **79**, 981-996.

Vanwaversveld J, Addink ADF and Vandenthillart G. (1989). The anaerobic energy-metabolism of goldfish determined by simultaneous direct and indirect calorimetry during anoxia and hypoxia. *J Comp Physiol B* 159: 263-268.

Wilson, J. M. and Laurent, P. (2002). Fish gill morphology: Inside out. J Exp Zool **293**, 192-213.

Wilson, J. M., Laurent, P., Tufts, B. L., Benos, D. J., Donowitz, M., Vogl, A. W., and Randall, D. J. (2000). NaCl uptake by the branchial epithelium in freshwater teleost fish: an immunological approach to ion-transport protein localization. J Exp Biol **203**, 2279-2296.

Wood, C. M. (1993). Ammonia and urea metabolism and excretion. In The Physiology of Fishes (ed. D. H. Evans), pp. 379-425. Boca Raton: CRC Press.

Wood, C. M., Gilmour, K. M., Perry, S. F., Part, P., Laurent, P., and Walsh, P. J. (1998). Pulsatile urea excretion in gulf toadfish (Opsanus beta): Evidence for activation of a specific facilitated diffusion transport system. J Exp Biol **201**, 805-817.

Wood, C. M., Kajimura, M., Sloman, K. A., Scott, G. R., Walsh P. J., Almeida-Val, V. M., and Val, A. L. (2007). Rapid regulation of Na+ fluxes and ammonia excretion in response to acute environmental hypoxia in the Amazonian oscar, Astronotus ocellatus. Am J Physiol Regul Integr Comp Physiol **292(5)**, 2048-2058.

Wright, P. A. (1995). Nitrogen excretion: three end products, many physiological roles. J Exp Biol **198**, 273-281.

Wu, R. S. (2002). Hypoxia: from molecular responses to ecosystem responses. Mar Pollut Bull **45 (1-12)**, 35-45.

Yan, J. J., Chou, M. Y., Kaneko, T., and Hwang, P. P. (2007). Gene expression of Na^+/H^+ exchanger in zebrafish H^+ -ATPase-rich cells during acclimation to low-Na^+ and acidic environments. Am J Physiol **293**, C1814-C1823.

Zall, D. M., Fisher, M. D., and Garner, Q. M. (1956). Photometric determination of chloride in water. Anal Chem **28**, 1665-1678.